Oxidative dissolution of hydrothermal mixed-sulphide ore: An assessment of current knowledge in relation to seafloor massive sulphide mining

Emily K Fallon[1,3], Dr. Sven Petersen[2], Dr. Richard A Brooker[3], Dr. Thomas B Scott[1],

[1] Interface Analysis Centre, School of Physics, HH Wills Physics Laboratory, Tyndall Ave. University of Bristol, BS8 1TL. UK.

[2] GEOMAR, Helmholtz-Zentrum für Ozeanforschung Kiel
Wischhofstr. 1-3, Geb.8A, Raum 107
24148 Kiel, Germany

[3] School of Earth Sciences, Wills Memorial Building, Queens Rd, University of Bristol, BS8 1RJ. UK.

*Current address to which correspondence should be sent; Interface Analysis Centre, School of Physics, HH Wills Physics Laboratory, Tyndall Ave. University of Bristol, BS8 1TL. UK.
Tel. (44) 117 3317685
Email. e.fallon@bristol.ac.uk

Abstract

The weathering process of seafloor massive sulphide (SMS) deposits can be considered analogous to weathering of terrestrial volcanogenic massive sulphides (VMS) deposits. However, in the context of SMS deposits, the process occurs in chemically buffered waters of near neutral pH, resulting in the formation of insoluble Fe oxy-hydroxide minerals including goethite and hematite as well as sulphates such as jarosite. As a result of this precipitation, it is commonly assumed that any SMS deposit is unlikely to exhibit a significant loss of metals (dissolution and release of heavy metals) into the water column. However, galvanic interactions have never been considered in this seafloor context, whilst they have already been shown to have the ability to increase dissolution significantly in terrestrial deposits. If heavy metal release is not temporally balanced by precipitation of oxide phases, there is the potential that these metal occurrences lose economic value. This is specifically significant if there is an

industrial focus on exploiting deposits associated with hydrothermal vents that have been inactive for some time. Not only this, but the geochemistry of weathering products - 'gossans' - that are formed have the potential to be used as tools for exploration. Furthermore, it is unknown what impact galvanic coupling may have with regards to anthropogenic release of heavy metals during seafloor mining of deposits associated with either active or inactive vents (disturbance of sediment, plume generation and dewatering process). This environmental impact needs to be addressed prior to the formulation of regulations for deep-sea mining by the International Seabed Authority.

The present review examines our current understanding of oxidation and dissolution of a mixed sulphide ore, bringing together lines of evidence from a range of literature sources. Based on this review, different seafloor sulphide ore deposits will dissolve by oxidation and release a variety of different metals (economic and/or toxic), all at different rates, with galvanic cells playing a role by increasing dissolution rates. While precipitation of oxide and oxy-hydroxide phases will occur, it is unknown in both a natural weathering and anthropogenic (mining) context whether heavy metal release (including economic and toxic metals) is temporally balanced by this precipitation and any subsequent adsorption. Based on our current understanding, certain sites will be more predisposed to oxidation as a result of their mineralogy (those containing significant pyrrhotite, marcasite, galena and secondary copper sulphides) and/or environment (higher temperatures and oxygen concentrations, lower pH's). Furthermore, certain sites pose more of an environmental risk (in terms of toxicity) than others, with arc-related SMS deposits associated with higher concentrations of As, Pb, Sb, Cd and Hg and ultra-mafic hosted SMS deposits associated with high concentrations of Co and Ni. The review highlights the need for subsequent studies that investigate the natural weathering process of seafloor sulphide ore deposits, including how this process impacts their economic value and consequent geochemical signature of oxides that are produced over time. Moreover, this review underlines the necessity for experiments to elucidate the oxidative dissolution of ore throughout any mining process.

Keywords

SMS deposits

Oxidation

Galvanic Cells

Metal release

Economic potential

Mining impact

1 Introduction

Whether associated with active or inactive hydrothermal vents, there is an interaction between sulphide minerals on the seafloor and oxygenated seawater that results in oxidative weathering (Edwards, 2004). Continued circulation of oxygenated seawater throughout the deposit via fractures and faults, will ultimately result in its slow destruction unless the deposit has been preserved and protected from oxidation by volcanic or sediment cover (Ridley, 2012). However, there is also some potential for intermediate supergene enrichment by the replacement of primary sulphides with secondary sulphides and gossans (Hannington et al., 1988; Herzig et al., 1991).

A similar process of weathering occurs in terrestrial analogues, better known as volcanogenic massive sulphide (VMS) deposits. Unlike their oceanic counterparts, weathering typically results in a low pH (<3) and can result in acid rock drainage (ARD), which strongly promotes further dissolution rather than a protective barrier. This is shown in Equations 1.1 and 1.2 involving pyrite.

Equation 1

$$FeS2+3.5O2\ aq+\ H2O \rightarrow\ Fe2++\ 2SO42-\ +2H+$$

Equation 2

$$FeS2+14Fe3++8H2O \longrightarrow 15Fe2++2SO42-+16H+$$

The main difference is that weathering processes on the seafloor occur in waters

of near neutral and buffered pH and the reaction results in formation of insoluble Fe-oxide and Fe-oxyhydroxide minerals such as goethite and hematite as shown by Equations 1.3 and 1.4 involving pyrite. These minerals can accumulate as insulating crusts or caps on the seafloor sulphide deposits, sometimes up to several tens of centimetres thick (Hannington and Jonasson, 1992) and are referred to as 'gossans' (Herzig and Hannington, 1995). Furthermore, the huge dilution factor and presence of numerous buffers make it unlikely that any significant net acid generation would occur (i.e., ARD as is known in a terrestrial context).

Equation 3

$$2FeS2 + 7.5O2\ aq + 4H2O \rightarrow Fe2O3 + 4SO42- + 8H+$$

Equation 4

$$FeS2 + 3.75O2aq + 3.5H2O \rightarrow Fe(OH)3 + 2SO42- + 4H+$$

In addition to the insoluble Fe oxyhydroxide minerals, copper weathering products have also been observed at SMS deposits. In particular, atacamite, paratacamite and botallackite ($Cu_2Cl(OH)_3$) have been identified at the Trans-Atlantic Geotraverse (TAG) and Logatchev, Mid-Atlantic Ridge sites (Dekov et al., 2011; Hannington, 1993). It is important to note that some of these secondary minerals (weathering products) are formed as a result of acidic pore waters (atacamite, jarosite) and not only from reaction with neutral pH seawater.

Fe-oxides and Fe-oxy-hydroxides have been shown to adsorb heavy metals and therefore can also behave as a sink for metals during sulphide dissolution as well as forming a protective crust on a deposit, physically inhibiting further oxidative weathering (Benjamin and Leckie, 1981; Bruemmer et al., 1988). Dekov et al. (2011) show that Cu weathering products such as atacamite and paratacamite from Logatchev vent field at 14°45'N on the Mid Atlantic Ridge, do not behave as sinks for heavy metals during weathering via adsorption, evidenced by their depletion in trace metals (Au, Ag, Co, Ni, Zn). In contrast, gossans associated with atacamite from TAG hydrothermal field at 26°N on the Mid Atlantic Ridge are Au

enriched compared to others in the same area (Hannington et al., 1988; Herzig et al., 1991), although it is suggested the gold is present as native Au grains, rather than within the lattice of atacamite.

In general the production of Fe-oxides and Fe-oxy-hydroxides, with their ability to act as a sink for metals, suggest it is unlikely that there will be any substantial loss of metals (dissolution and release of major metals including Fe and Cu) into the sea. However, mobilisation is possible, where atacamite has been observed in sediment samples without significant sulphides at Logatchev, indicating limited transport of Cu away from sulphides (Dekov et al., 2011). ARD would be a possible way to release the metals in confined areas on land, but in this deep-sea context with the high dilution factor and buffering nature of seawater, ARD would be highly unexpected as a major process.

Another mechanism for metal release that has received little attention is galvanic interaction. SMS deposits include a variety of intimately associated sulphides, and it is the galvanic interaction between such minerals and inclusions that might have the ability to substantially increase the release of metals into the water column via increased dissolution (Abraitis et al., 2004a; Da Silva et al., 2003; Heidel et al., 2013; Koleini et al., 2010; Kwong et al., 2003; Li et al., 2006; Liu et al., 2008; Mehta and Murr, 1983). If the increased rate of metal release due to galvanic interactions is not balanced by precipitation of phases, there is the potential for release of toxic metals into the water column. Subsequent metals may bioaccumulate in local ecosystems, disperse or accumulate in the wider ocean or ultimately precipitate out elsewhere as oxides. If this process is already happening naturally it could be reducing the economic worth of deposits, but if the galvanic reactions are mechanically accelerated by any future mining activity at SMS deposits, there is increased potential for heavy metal release into the sea.

The aim of this review is to bring together lines of evidence that will help us to understand this natural weathering and oxidation process, how galvanic interactions may play a role and how this natural process could be intensified through mining. It also aims to highlight the areas where understanding is lacking

and suggestions on how this can be improved in the future.

2 Mining of SMS Deposits

2.1 Economic worth of SMS deposits associated with inactive hydrothermal vents

Hannington et al. (2010), Hannington and Jamieson (2011) and more recently, Monecke et al. (2016) discuss the economic potential of modern seafloor massive sulphide ore deposits with respect to metal grades and tonnage. They further state that those metal accumulations that are associated with inactive vents with no major sediment cover will greatly reduce the environmental impact and therefore be of higher economic interest. It has also been suggested that occurrences on slow spreading ridges tend to be larger, and those associated with ultramafic host rocks are richer in Cu (>10 wt%) and Au (>3 ppm) (German et al., 2016; Hannington et al., 2011).

Plume signal detection is used to identify the location of hydrothermal vents and any associated SMS deposits. However, as this technique is limited to active vents only, the majority of estimates of the total number of SMS deposits are assumed to be underestimates where they do not include extinct deposits (deposits associated with inactive hydrothermal vents) (Hannington et al., 2010). Current exploration methods ultimately make it difficult to identify inactive deposits and there is a high demand for an inventory of inactive deposits (Hannington et al., 2010). The resource potential of SMS deposits associated with inactive vents is unknown but is thought to be high, with suggestions that inactive sites are ten times more abundant than active ones (Murton, 2013). Hannington et al. (2011) state that if present-day rates of SMS formation on ridges are extrapolated, significant tonnages may be expected off-axis, making such areas a preferred target for future metal extraction.

Although the natural weathering process has been studied (Edwards, 2004; Edwards et al., 2003; Toner et al., 2008), it has never been fully considered in terms of how it might deplete the economic value of a deposit over time. The oxidative weathering of both terrestrial and seafloor hydrothermal sulphides to

produce ’gossans’ (Herzig and Hannington, 1995), has the potential for release of economic metals. At TAG and Logatchev, gossans contain abundant Fe oxy-hydroxides (goethite and hematite), secondary Cu sulphides, jarosite and secondary copper minerals including atacamite (Dekov et al., 2011; Hannington, 1993).

The effect on economic value depends upon the distribution of metals throughout the weathering process, and whether or not metals are i) leached and lost, or ii) retained either in the primary sulphide or iii) retained in the secondary weathering products. This in turn also affects whether or not the geochemical composition of the overlying oxides might be utilised as a tool for exploration. The weathering process of sulphide minerals is complex and varies as a function of primary mineralogy, porosity, grain size, reactive surface area, time, temperature, pH, Eh amongst others. Numerous studies have discussed and analysed the retention of elements throughout the weathering process for terrestrial sulphide ore (Atapour and Aftabi, 2007; Thornber, 1985; Thornber and Wildman, 1984). In general the assessment of economic worth of a weathered seafloor sulphide ore deposit is very limited (Hannington et al., 1988; Herzig et al., 1991). In some respects, the extent of weathering is of secondary importance in comparison to the overall size of the deposit although it might become important for older deposits or if some particular metal is the target. It is probably the case that the primary sulphide deposit will have reduced in size, but metals such as Fe and Cu are retained as they are either converted to a weathered sulphide ore containing secondary sulphides or a completely oxidised ’gossan’ deposit. However, the behaviour of other individual trace metals (Zn, Pb, Sb, Cd, Tl, Hg, Se, Te, In, Ge and Ga) becomes an important consideration (Monecke et al., 2016).

Secondary sulphides are the product of either hydrothermal fluid-seawater mixing or the initial stages of seafloor oxidation or primary sulphide minerals, and can be enriched in base (Cu) and precious metals (Au, Ag) due to leaching and re-deposition (Hannington et al., 1988). As demonstrated by Herzig et al. (1991), secondary sulphides from TAG contain predominantly Cu sulphides and jarosite with economically significant concentrations of metals, showing an average of 9.1 ppm Au, 62 ppm Ag, 24.60 wt % Cu and 1.23 wt % Zn. It is thought that this initial

weathering (including the formation of secondary copper sulphides) can occur when temperatures and pH have not reached that of ambient seawater, but are still generally considered ‘lower temperature’ (Hannington, 1993; Rouxel et al., 2004).

Subsequent to this initial weathering, it is suggested that over extended periods, Au and Cu are dissolved by the relatively isolated acidic pore fluids (generated by reaction of sulphides and seawater) (Hannington et al., 1990), transported as $CuCl^{4-}$ and $AuCl^{4-}$ complexes (Thornber, 1985) and then re-deposited once mixed with fresh seawater (Herzig et al., 1991) as the acidity is diluted. The final ’gossan’ product includes Fe-oxide, jarosite +/- atacamite, depending on the parental sulphide assemblage.

Herzig and Hannington (1991) analysed Fe-oxide gossans that have developed at the edge of the TAG Hydrothermal Field, that started to form 40-50,000 years ago (Lalou et al., 1990) and have since been weathering. The study shows that where Cu, Zn, Ag, Sb, and Au are present in the primary ‘parent’ sulphide, they have the potential to be preserved within a gossan. Significant concentrations of gold (4.68-23.00 ppm) and enrichments in Ag, Sb and Mo were observed in atacamite bearing (Cu-rich: 20-40 wt%) Fe-oxide gossans. However, it is apparent that these gossans can be ’fertile’ or ’barren’. Au-poor gossans were also observed and shown to have a sulphide origin. Nonetheless, based on the minimal observed atacamite, it is suggested that the parent sulphide this gossan originated from was unlikely to have been initially endowed with Cu and Au. Au-poor gossans were shown to be associated with significantly higher concentrations of Fe-oxide, SiO_2, As, Zn and Co in comparison to Au-rich gossans.

This and the findings from both Hannington et al. (1988) and Herzig and Hannington (1991) raise the prospect that other seafloor gossans may contain significant concentrations of recoverable gold similar to TAG. Further support is found in evidence of significant gold found in fossil seafloor gossans that are now present on land (Hannington et al., 1991). These studies indicate that the economic value of such deposits can clearly be retained during the course of

oxidation and weathering, although the way of recovering the same metal from a now different mineral assemblage may also have economic implications.

2.2 Environmental impact of mining

The process of deep-sea mining has the potential to expose a high surface area of fresh sulphide minerals to the corrosive effects of seawater, allowing for additional oxidative dissolution (Gwyther, 2008a). Material released during the extraction process or waste water return from dewatering the slurries at the surface, will be suspended in the water column as a sediment plume to be either dispersed into wider ocean and ultimately to settle out some distance away. During either process, this fine suspended sulphide particulate has the ability to dissolve, releasing heavy metals and toxins into the water column and thereby having a detrimental impact on the local ecosystems (Boschen et al., 2016, 2013, Van Dover, 2014, 2010, 2007). For accumulation or dispersion throughout the wider ocean, the impact is presumed to be limited as a result of the large dilution factor. However the important consideration is the detrimental impact to the local environment and associated ecosystems.

During mineral processing and dewatering at the surface, there is the potential for exposure of sulphide to higher oxygen concentrations and higher temperatures, contributing to enhanced dissolution. Nautilus Minerals Ltd provide the only current concept for the mining of hydrothermal vents. Based on information in the Environmental Impact Statement (EIS), any exposure to higher oxygen concentrations and temperatures will be brief (<30 minutes). Of more concern, is that this return water will include solid material <8 μm in diameter with an expected total dissolved solids (TDS) of 6,350 mg/L (Gwyther, 2008a). These suspended sulphide particles (TDS) within this returned seawater would be available for reaction upon its return to the seafloor, potential releasing more metals. Given the expected TDS above and assuming cube-shaped pyrite; for particles of either 0.1 μm or 8 μm in size, the surface area of the TDS would be 3.81×10^{14} or 4.76×10^{12} μm^2 respectively.

It has been suggested in several studies that there is the potential for localised

acid generation during the anthropogenic oxidative dissolution of sulphide ore deposits creating local acid rock drainage (Bilenker, 2011; Romano, 2012). This localised acid generation during the weathering process is supported by observations of atacamite (Dekov et al., 2011; Hannington, 1993) and jarosite in weathered SMS deposits (Hannington and Galley, 1998). However, in terms of acid generation from in situ SMS mining, a recent study by Bilenker et al. (2016) uses sulphide dissolution rates to suggest that any acid production would be insufficient to exceed the buffering capacity of advecting seawater that would be expected in a mining environment.

The global issue of ocean acidification has the potential to be a cause for concern in this context. Global mean surface ocean pH has decreased by 0.1 pH unit since pre-industrial times and is projected to drop another 0.3-0.4 pH units by the end of the century (Caldeira and Wickett, 2003; Cao et al., 2014; Feely et al., 2009; Guinotte and Fabry, 2008) as a result of rising atmospheric CO_2. The evolution of mean surface pH is difficult to predict and is largely dependent on the rate at which atmospheric PCO_2 change increases (Hönisch et al., 2012). Changes in deep ocean chemistry generally lag behind the change in atmospheric CO_2 and surface ocean pH as a result of the long time scales (geological timescales) required for penetration of excess CO_2 into the deep ocean (Cao et al., 2014; Guinotte and Fabry, 2008; Levin and Le Bris, 2015). It is therefore expected that the full effects of ocean acidification will not be observed in the deep ocean for years to come and are unlikely to be of any concern within the context of deep sea mining in the next 100 years. Nonetheless, there should be a future concern in regards to any mine waste that is placed on the seafloor where exposure to the projected changes in deep ocean pH has the potential to enhance dissolution.

2.2.1 Ecological risk

A release in Cu, Zn, Cd, Hg, As, Pb, Te, Se, Ag, Co, Ni from dissolving minerals all have the potential to negatively impact vent ecosystems, with Cu, Zn, Hg and Cd perhaps posing the most risk (Ando et al., 2002; Jeanthon and Prieur, 1990; Llanos et al., 2000; Nies, 1999; Vetriani et al., 2005). It has been speculated that any high concentrations of heavy metals that are released by an active hydrothermal vent or through oxidation on an active vent will pose minimal risk to

the fauna that have adapted to live at that site (Ando et al., 2002; Edgcomb et al., 2004; Gwyther, 2008a; Jeanthon and Prieur, 1990; Llanos et al., 2000; Rathgeber et al., 2002; Vetriani et al., 2005).

It has been suggested among the scientific community that the environmental and ecological risk of mining will be significantly reduced if inactive deposits are mined (Drew, 2009; Herzig, 1999). Recent research at inactive vents shows that the 'vent' type animals are absent (Erickson et al., 2009). Kato et al. (2010), demonstrate that the microbial diversity at inactive vents is in reality comparable, or in some cases, higher than that seen on active vents whilst having significantly less biomass. It is important to note that whilst the diversity of macro fauna tends to be higher at inactive vents (Boschen et al., 2013), this diversity is not endemic to inactive deposits (Van Dover, 2010) and is therefore less vulnerable to habitat loss compared to active vent species that are highly specialised extremophile communities.

There are still risks with mining inactive vents: ecosystems are primarily at risk from destruction of their energy source (the ore deposit itself), suffocating sediment plumes and the toxic nature of any plume or material dissolved as a result of extraction. Impact can still be high as background fauna have been shown to have slower growth rates than the active vent species and thus the recovery times from disturbance are likely to be greater (Van Dover, 2010). Furthermore, fauna at inactive sites have shown to be sensitive to toxic metals (Hg) in comparison to those that are adapted to active vents (Vetriani et al., 2005). Ultimately the literature demonstrates the difficulty in determining whether the vent ecosystem and its diversity are a function of the presence of vent fluid, substrate weathering, substrate composition (mineralogy) or a combination of these (Suzuki et al., 2004).

It has been hypothesised that, next to the chemosynthetic hydrothermal vent fauna and the background fauna, there is a third community that include fauna that are specially adapted to the weathering of inactive deposits (Boschen et al., 2013; Van Dover, 2007). If this is found to be the case, the impact to this

ecosystem could be significant, unless the recovery rate of such a habitat is high.

2.3 Seafloor gossans

2.3.1 A tool for detection?

There has been a significant drive to find new tools for detection and identification of both active and inactive hydrothermal vents and their associated sulphide ore deposits. Most have focused on active vents, primarily due to the relative ease of finding them with their distinctive thermal and chemical plumes, but inactive vents, although thought to be more numerous (Murton, 2013), are more difficult to locate (Monecke et al., 2016).

With respect to the exploration for inactive deposits, research is focused on geophysical techniques (Kowalczyk, 2011) including magnetic (Dyment et al., 2011; Tivey and Dyment, 2013), gravity (Kinsey et al., 2008), resistivity (Wolfgram et al., 1986) and self potential surveys (Cherkashev et al., 2013). In addition, 'in situ' versions of geochemical techniques including Raman spectroscopy (White, 2009; White et al., 2005), luminescence and XRF (x-ray fluorescence) also have potential. Geophysical surveys such as magnetic and gravity surveys obviously have the advantage for detecting deposits as they do not require being positioned on the seafloor and certainly have the ability to cover more ground in a certain time period and to detect deposits under a few meters of cover rocks (lavas or sediments).

For terrestrial sulphide ore deposits, natural acid rock drainage products or ’gossans’ are extensively used as an exploration tool (Bull and Mazzucchelli, 1974; Taylor and Thornber, 1992). A combination of mineralogy, texture, field relationships and geochemistry is used to identify a ’fertile’ gossan - a gossan that is associated with base metal sulphide ore deposits and discriminate against ’barren’ gossans. In a similar way, weathering products and oxide coatings associated with inactive SMS deposits can be utilised as an exploration tool. This is mainly achieved by sediment coring, where gradients in geochemical anomalies can be used to predict the location of SMS deposits, or by visual methods, where

the coloration of the surface sediments guides exploration. Currently no fast, remote technique exists that can detect and identify such material 'in situ' on the seafloor.

In theory, the geochemistry of a gossan can be utilised to determine the nature of mineralisation at depth as long as trace elements that are present in the primary sulphide ore are retained throughout oxidation and survive in the weathered deposit (gossan). Whether a given element survives the weathering process is dependent on numerous physical and chemical conditions and in this context include topographic relief, seawater conditions (pO2, T, salinity, composition), permeability/porosity, pH and Eh of porewaters, nature of host rocks and type of mineralisation (Taylor and Thornber, 1992). Utilisation of gossan geochemistry and the application to exploration has been discussed in numerous, but mainly terrestrial studies (Andrew, 1984; Atapour and Aftabi, 2007; Bull and Mazzucchelli, 1974; McGoldrick and Keays, 1981; Nickel, 1984; Taylor and Scott, 1982; Taylor and Thornber, 1992; Travis et al., 1976). In VMS mineralisation that is hosted by felsic volcanics, Cu, Pb, Ag, Au, As, Sb, Bi, Se, Hg, Sn and Ba are found to be useful in identifying fertile gossans (Taylor and Thornber, 1992).

In many ways it is likely that SMS gossans on the seafloor will be more persistant and easier to interpret as an exploration tool than their terrestrial counterparts. They are always formed as soon as the sulphides are exposed to seawater, always preserved (due to the buffering and oxidising potential of seawater) (Hekinian, 2014) and the environment of formation is likely to be similar across the globe in terms of pH, due to the buffering capabilities of seawater. However, local temperature, Eh, pressure and initial mineralogy may vary significantly and, unfortunately, Fe oxide/oxy-hydroxide minerals are not unique to sulphide ore deposits. Similar to terrestrial sulphide ores, there is still a need to discriminate between ’gossans’, ’ochres’ and Fe-oxy-hydroxide deposits formed by different processes as highlighted in Table 1.

There have only been two studies investigating geochemical signatures in seafloor gossans (Barrett et al., 1990; Herzig et al., 1991). Both investigate REE

signatures, with barite in gossan caps from the Southern Explorer Ridge retaining a REE signature linked to high temperature solutions (Barrett et al., 1990) and Fe-gossans from TAG and ochres from Skouriotissa, Cyprus displaying similar REE signatures that are likely retained from the primary sulphide (Herzig et al., 1991). Further to this, concentrations of Au, Cu, Sb, Co and Se in Au-rich gossans from TAG are similar to those in secondary sulphides (digenite, covellite), indicating inheritance of this geochemical signature from the parent sulphide ore (Hannington et al., 1991). Gossans where gold concentrations were found to be low (average of 0.15 ppm) do contain base metals (>1% Cu and Zn) and jarosite, confirming they also have a primary sulphide origin but the very minimal atacamite suggests that they are derived from a different, low Cu parent sulphide, which was also low in Au. Both observations suggest that it is the parent sulphide that dictates the chemistry of the subsequent weathering products but it is ultimately difficult to determine the conditions during weathering as well as rule out the potential presence of an outside source of Au-poor Fe oxides/oxy-hydroxides. For example, Au-poor Fe-oxy-hydroxides can also be formed by low temperature hydrothermal fluids or by plume fallout; both contributing to the gossan formation (see Section 2.2) (German and Sparks, 1993; Mills et al., 1993). Furthermore, there is potential for Fe oxides and oxy-hydroxides that have formed to be adsorbing metals from seawater (see Section 2.3.2). This can subsequently alter their geochemistry, making it difficult to pinpoint the geochemical source: dissolving parent sulphide or seawater, or most likely: both.

It should always be remembered that given the small size of seafloor sulphide ore deposits, even if a 'fertile' gossan is observed, it will not guarantee the presence of a metal-rich sulphide ore deposit beneath, nor will it have any meaning for the size of the underlying deposit. Further to this, any underlying sulphide deposit could be fully weathered to oxides, depending on the original size and age of the deposit. If this is the case, and the primary sulphide is completely oxidised, based on these limited studies, gold may still be present in the gossan but base metals including Zn may not. This leads to several questions. How and what metals are retained? Are weathering products including atacamites stable over long periods or do they themselves alter or dissolve over time? Hannington (1993) shows that only freshwater will dissolve atacamite, resulting in

the lack of atacamite in fossil deposits on land, however investigations of the solubility and stability of atacamite have focused on the low pH (4 to 5), ambient (25°C) and high (25 to 500°C) temperature range (Le Roux et al., 2016; Pollard et al., 1989; Sharkey and Lewin, 1972). Hannington (1993) highlights the instability of a specific polymorph of atacamite: botallackite, in TAG gossans, but there have been no studies on the solubility of atacamite at lower temperatures and higher pH.

2.3.2 A sink for toxic metals?

As highlighted in the previous section, Fe oxides and gossans have been shown to retain metals, including those that could be environmentally and ecologically significant if released in high concentrations during mining. Whilst iron and copper appear to be retained, forming secondary minerals, other metals that may be present within the lattice of sulphide minerals have the potential to be released. It has been shown in the literature that there is a high capability for adsorption of heavy metals (Cd, Zn) onto amorphous iron oxy-hydroxides (Benjamin and Leckie, 1981) and goethite (Bruemmer et al., 1988) suggesting that they may be an effective sink for trace metals.

Benjamin and Leckie (1981) show that adsorption is pH dependent where adsorption increases from zero to hundred percent within a narrow band of pH. The narrow band of adsorption is specific to an individual metal and ranges significantly depending on the metal in question. There is also a pH dependency upon diffusion rates for adsorption of metals where different metals adsorb at different rates. This adsorption effect has been documented on the seafloor in regards to the formation of cobalt rich ferromanganese crusts (Hein et al., 2013) where precipitated colloids of iron oxides acquire trace metals including U, Th, Pb, Hf, Mo and Co.

This adsorption effect has the potential to minimise the release of metals into the seawater. However, whether the adsorption of trace metals onto these secondary minerals can keep up with any release from anthropogenic dissolution is unknown.

3 Experimental investigation of oxidative dissolution

The mechanism of oxidation of sulphides - pyrite in particular - has been extensively studied (Bierens de Haan, 1991; Evangelou and Zhang, 1995; Holmes and Crundwell, 2000; Long and Dixon, 2004; McKibben and Barnes, 1986; Moses and Herman, 1991; Nicholson et al., 1988; Rimstidt and Newcomb, 1993; Rimstidt and Vaughan, 2003; Wiersma and Rimstidt, 1984; Williamson and Rimstidt, 1994). A review by Chandra and Gerson (2010) highlights the debate amongst the literature between a chemical or electrochemical process for pyrite oxidation, with general acceptance of an electrochemistry dominated oxidation process (Chandra and Gerson, 2010; Gartman and Luther, 2014).

3.1 Individual sulphide minerals

Whilst dissolution studies of specific minerals in seawater have been undertaken (Bilenker, 2011; Bilenker et al., 2016; Feely et al., 1987; Morse, 1991; Romano, 2012), the majority of published data are within the context of terrestrial acid mine drainage arising from mine flood and leaching of tailings piles by meteoric waters and are only discussed in terms of trends (not absolute rates) for the purposes of this review (Acero et al., 2009, 2007; Bonnissel-Gissinger et al., 1998; Constantin and Chiriţă, 2013; Descostes et al., 2004; McKibben and Barnes, 1986; Moses et al., 1987). Rates are affected by temperature, pH, salinity, oxidising agents and their concentration, flow rate, grain size, surface area, pressure and impurities. Impurities in particular have been shown to play a major role, which is significant (see galvanic coupling section).

In the study of Feely et al. (1987) the abiotic dissolution rates determined for sulphide minerals (pyrrhotite, pyrite, marcasite, sphalerite, chalcopyrite) in seawater vary by over three orders of magnitude as shown in Table 2. Other seawater dissolution rates for sulphide minerals (Morse, 1991; Bilenker et al., 2011; Romano, 2012; Bilenker et al., 2016), have been derived using different methods, and where possible have been re-calculated for comparison in Table 2. Dissolution rates by Feely et al. (1987) are calculated by mass change over time and expressed as cm s^{-1} whereas Bilenker (2011) and Romano (2012) derived

molal specific rate laws using concentrations of Fe and Cu released into solution over time which is expressed in moles per kg per s. Calculations are presented in Appendix A.

Sulphide dissolution rates (cm s^{-1}) versus temperature derived by Feely et al. (1987), Morse (1991), Bilenker (2011) and Romano (2012) are shown in Figure 2, where rates are presented in these units in order for comparison between studies. When comparing similar run conditions (PO_2, pH and temperature), it can be observed that the oxidation rate of pyrrhotite is approximately two orders of magnitude faster than chalcopyrite. Field dissolution rates of chalcopyrite (Feely et al., 1987) are comparable to those of Bilenker (2011), whereas field dissolution rates of pyrrhotite (Feely et al., 1987) are two orders of magnitude faster than those of Romano (2012). Both point toward a much faster oxidation rate of pyrrhotite over pyrite and chalcopyrite. Feely et al. (1987) rates suggest that pyrrhotite, marcasite and sphalerite oxidise at least one order of magnitude quicker than chalcopyrite; in particular they show that marcasite can show complete dissolution within a few hours to a few weeks of formation. Reported dissolution rates of pyrite are conflicting with field studies by Feely et al. (1987) showing slow rates (although still two orders of magnitude faster than chalcopyrite) whereas lab based rates by Feely et al. (1987) and rates by Morse (1991) are much faster. Lab based rates for pyrite are three orders of magnitude faster than chalcopyrite and those by Morse (1991) range from three to four orders of magnitude faster than chalcopyrite.

Whilst no specific oxidation rates have been derived for secondary copper sulphides (chalcocite, covellite, bornite, enargite, tennantite), through the study of zeta potential and XPS analysis, Fullston et al. (1999) were able to provide a ‘ranking’ of oxidation: chalcocite > tennantite > enargite > bornite > covellite > chalcopyrite, with chalcocite oxidising at a faster rate.

Sulphides including pyrite, marcasite, chalcopyrite, sphalerite and galena are electron semiconductors, with their semiconductor properties resulting from free charge carriers arising from variations in stoichiometry and trace elements

within the mineral lattice. The defects found in the crystal site which produce the carriers can be distinguished based on whether they donate electrons (n-type) to the conduction band, providing excess electrons to the semi-conductor, or whether they accept electrons (p-type) from the valence band, leaving excess holes in the semi-conductor. Unless the concentrations of donors and acceptors is equal, semi conductors can be characterised as either n-type or p-type according to which carriers dominate (Pridmore and Shuey, 1976).

Sulphides formed at hydrothermal vents on the seafloor are generally polymetallic, non-stoichiometric and contain a range of lattice impurity trace elements (Abraitis et al., 2004a; Beaudoin, 2000; Chen et al., 2010; Johan, 1988; Lepetit et al., 2003; Si et al., 2006; Tong et al., 2006). It has been reported in numerous studies that the impurities within sulphides significantly influence the electrochemical and semi-conducting properties (p or n type semi-conductor) and ultimately their environmental reactivity and oxidation/dissolution behavior (Becker et al., 2001; Biegler, 1976; Chandra and Gerson, 2010; Chen and Chen, 2010; Ellmer and Höpfner, 2006; Harmer et al., 2008; Hu et al., 2010; Oertel et al., 1999; Richardson et al., 1994; Savage et al., 2008). This has mainly been studied by the mining industry as this reactivity of sulphides affects flotation, separation and concentration of ores. Not only do these impurities influence their individual semi-conducting properties but also their rest potentials which ultimately affects their interaction with other minerals in terms of galvanic cells (see galvanic coupling).

Understanding the impurity content of sulphides is imperative to understanding their subsequent oxidative dissolution. By considering the trace elements constituent within sulphide minerals, particular sulphide ore deposits can be identified as more or less reactive and provide an accurate assessment of toxic metal release potential. Characteristics of a deposit that affect its oxidation and dissolution potential can be identified, allowing development of strategies for dealing with mine waste and remediation.

3.1.1 Pyrite & Marcasite

Pyrite and marcasite are polymorphs of FeS_2, the former being cubic, the latter

forming a metastable orthorhombic crystal structure making it very brittle and subject to 'pyrite decay' even in air. The semi conducting properties of pyrite have been shown to vary by four orders of magnitude (Abraitis et al., 2004b) produced by variations in stoichiometry and the abundance of trace metals within the pyrite (most commonly As, Co and Ni, but can also include Zn, Tl, Sb, Pb, Mo, Hg, Cu, Bi, Au, Ag) (Chandra and Gerson, 2010; Ellmer and Höpfner, 2006; Gupta et al., 1980; Liu et al., 2007; Lowson, 1982; Oertel et al., 1999; Rimstidt and Vaughan, 2003; Savage et al., 2008). Pyrite can be characterised as either primary p-type or n-type semiconductor by both stoichiometry and trace elements. A common criterion using trace elements is the method used by Wei (1996; Abraitis et al. (2004); Lehner et al. (2007); Liu et al. (2007) using the ratio of trace metal concentrations of As, Sb, Co and Ni:

Equation 5

$$\frac{[As]+[Sb]}{[Co]+[Ni]}$$

Where n-type pyrite semi-conductors are commonly found to contain high concentrations of Co and low concentrations of As whereas p-type have been shown to contain high As (Abraitis et al., 2004b; Savage et al., 2008).

Without the influence of trace element defects, stoichiometry can be used to characterise the type of semi-conductor where pyrites that have a stoichiometric S:Fe ratio of less than 2 (S-deficient) are generally found to be n-type and those above 2 are p-type. Interestingly, pyrite formed at high temperatures are generally n-type, with p-type more common at low temperatures (Abraitis et al., 2004b; Lowson, 1982). This could be related to a high temperature S deficiency or association of Co at higher temperature, versus As at lower temperature. Ultimately it is difficult to attribute the change in type to either temperature itself or the associated incorporation of certain trace metals with temperature.

Although at low pH (2), Wiersma and Rimstidt (1984) have shown that oxidation rate constants are different for different pyrites (formed at high and low temperatures) and for marcasite, with high temperature hydrothermal and metamorphic pyrites having the highest reactivity, marcasite intermediate and low

temperature pyrite having the lowest. Feely et al. (1987)'s experiments were undertaken at higher pH where oxidation is more significant and likely to make a greater difference to the reactivity's of pyrite and marcasite (Wiersma and Rimstidt, 1984).

3.1.2 Pyrrhotite

Pyrrhotite has a non-stoichiometric composition with $Fe_{1-x}S$, with x ranging from 0 (FeS) to 0.125 (Fe_2S_8) (Belzile et al., 2004). The structure of pyrrhotite can vary significantly, with the least Fe-deficient (47.4 to 48.3 mol% Fe) types forming hexagonal and orthorhombic structures and greater Fe-deficient (46.5 to 46.8 mol% Fe) types being monoclinic (Belzile et al., 2004 and references therein). Orlova et al. (1988) show that hexagonal pyrrhotite is more reactive than monoclinic, but in reality it is rare to find pyrrhotite present in only one form (Arnold, 1967). Vanyukov and Razumovskaya (1979) found that oxidation rates increase with an increase in the S:Fe ratio of pyrrhotite.

Typical trace elements in pyrrhotite include Co, Ni, Cu, Mn, Pb, Sn, Ti, Cr, Se and Ag (Arnold, 1967; Cabri et al., 1985; Hawley and Nichol, 1961). How trace metal content in pyrrhotites effects oxidation rates has not been quantified, however Kwong (1993) observed (semi quantitatively), that monoclinic pyrrhotites with a higher trace metal content oxidised slower than those with lower. This is in contrast to a pyrrhotite oxidation study by Janzen et al. (2000) who found that neither the structure nor trace metal content of pyrrhotites had a systematic effect on pyrrhotite oxidation rates.

Within the context of seafloor massive sulphides, pyrrhotite is commonly observed to be oxidised and replaced by Fe oxides and oxy-hydroxides (Koski et al., 1985; Zierenberg et al., 1984). Such replacement is observed more often than for the other sulphide minerals (pyrite, chalcopyrite), suggesting either a quicker oxidation rate than other sulphide minerals and/or galvanic dissolution of pyrrhotite if in the presence of other sulphide minerals.

3.1.3 Chalcopyrite

Chalcopyrites are also known to contain impurities. Butler and Nesbitt (1999) show

enrichments of V, Ag, In, Te, Ba, Au, Pb and U within chalcopyrite in the wall of a black smoker chimney. Modern studies on the impact of impurities in chalcopyrite on its dissolution are very limited (Dutrizac and MacDonald, 1973; Linge, 1977). Shuey (1975) and Pridmore and Shuey (1976) demonstrate that most natural chalcopyrites are n-type conductors, as a result of a sulphur deficiency; however samples with higher copper content are more resistive.

In terms of individual chalcopyrite minerals from different sources and presumably different trace elemental chemistry, a couple of studies have been undertaken but show contrasting results. Warren et al. (1982) show that electrochemical oxidation of chalcopyrite (in 1M H_2SO_4 solution) from different sources can vary by two orders of magnitude. They attribute this variation to a range of impurities within the samples. Contradictory results from Biegler and Swift (1979) show that the source (and subsequent trace geochemistry) of chalcopyrite has minimal effect on the rate of chalcopyrite dissolution.

Dutrizac and MacDonald (1973) undertook a series of dissolution experiments (low pH) with a range of chalcopyrites, however the chalcopyrites were not pure minerals, but contained impurities of other sulphide minerals (as distinct from trace elements within the chalcopyrite lattice). The reactivity of chalcopyrite varies significantly, and it was postulated that this was a result of galvanic interactions related to the polymineralic nature of the samples. Linge (1977) furthered this work, and agreed that whilst different chalcopyrites do react very differently, this is not due to galvanic interactions but due to the presence of sulphide minerals influencing the diffusion rate of the lattice elements within the chalcopyrite. On the other hand, subsequent leaching tests with chalcopyrite from different sources undertaken by Dutrizac (1982), showed that when leaching rates were corrected for the amount of chalcopyrite in each particular sample, similar leaching rates (within 50%) were observed. Biegler and Swift (1979) suggested that this variation in reactivity between chalcopyrite samples is not necessarily due to semi-conductor effects, and that it is difficult to compare batch-leaching results with those arising from electrolysis studies.

3.1.4 Sphalerite

Typical trace elements in sphalerite include Fe, Cd, Mn, Cu, Co, Ni, Hg, Ga, Ge, Ag, In, Sn, Pb and Sb (Beaudoin, 2000; Chen et al., 2010; Johan, 1988; Lepetit et al., 2003; Si et al., 2006; Tong et al., 2006). Chen et al. (2010) undertook computational (density-functional theory) studies for sphalerite and show that Ag, Sn, Pb, Sb, Cd and Hg increased the conductivities of sphalerite, and that Mn, Fe, Ga, Ln, Sn and Sb changed the semi-conductor type of sphalerite from p-type to n-type. Overall, it was shown that Mn, Fe, Ni, Cu, Sn and Pb impurities favoured the oxidation of sphalerite, whereas Cd, Hg, Ga and In had the opposite effect (Chen et al., 2010). Chen et al. (2010) further showed the magnitude of effect the trace impurities had on oxidation of sphalerite, with high Fe sphalerite energetically favouring O_2 adsorption and being more easily oxidised (Fe: -181 kJ mol^{-1}) than Mn (-146.66 kJ mol^{-1}), Cu (-95.53 kJ mol^{-1}) and Cd (-55.96 kJ mol^{-1}), becoming harder to oxidise with the more positive O_2 adsorption energy. The results indicate that Fe enriched sphalerite is more reactive/easily oxidised and subsequently leached preferentially versus low-Fe sphalerite. These observations are consistent with numerous studies, including those of leaching experiments (Chandra and Gerson, 2010; Dutrizac et al., 2003; Gigowski et al., 1991; Harmer et al., 2008; Perez and Dutrizac, 1991; Weisener et al., 2004). The results also correlate with observations of an abundance of Fe-poor sphalerite in seafloor gossans by (Ridley, 2012) indicating a resistance to oxidation. The Fe content of sphalerites has not only shown to alter the mineral's reactivity, but also the rest potential (Majima, 1969) which can have significant impact when Fe-rich sphalerite is present with other sulphide minerals (see Galvanic coupling section).

3.1.5 Galena

Typical trace elements in galena include Ag, Cu, Zn, As, Sb, Bi, Cd, Tl, and In (Chen et al., 2011). Pridmore and Shuey (1976) suggest that donor defects related to Sb and Bi along with a deficiency in S make most galena n-type. Chen et al. (2011) undertook computational (density-functional theory) studies for galena and suggest that that trace impurities of Mn, As, Bi, In and Sb within galena change it from a p-type to an n-type semi-conductor. In particular, abundant trace impurities

of Mn and Sb in galena were shown to lead to an over-oxidation. In comparison, impurities of Ag, Cu, Zn, Tl and Cd were shown to have no effect on the type of semi-conductor (Chen et al., 2011).

3.2 Leaching of a mixed sulphide ore in seawater

Studies of leaching of a mixed sulphide ore in seawater are limited to two (Gwyther, 2008b; Rzepka et al., 2014). The most recent of which (Rzepka et al., 2014) was a study to evaluate the submarine (deep-sea) leaching potential of tailings from two terrestrial hydrothermal copper vein type deposits – Nussir and Ulveryggen (exploited by Nussir ASA) for the proposed tailings deposition in Repparfjorden, Norway. The deposits contain major bornite and chalcopyrite, as well as chalcocite and traces of covellite, with low pyrite content. Leaching tests were ran with 500g of sulphide ore, 2 L of natural filtered (0.2μm) seawater at a constant flow rate of 1-2 m/hr and oxygen saturation of 80-100%. The columns were run at ~10°C.

Perhaps more applicable to seafloor sulphide mining is the environmental impact study (EIS) for mining the Solwara 1 Deposit in Papua New Guinea (Gwyther, 2008b). There are two parts to that study, the first undertaken by CSIRO (Simpson et al., 2007) the second undertaken by Charles Darwin University (Parry, 2008).

This deposit is situated in an immature back-arc basin in the south-west Pacific Ocean. The specific mineralogy (modal abundance) of the samples was not presented for either the experiments of Parry, (2008) or Simpson et al., (2007), although the overall chemistry was provided and is reproduced in Table 4. Based on this chemistry, the mineralogy is substantially different between each of their experiments. Data from Parry, (2008) uses predominantly Fe-rich samples (31.6 % Fe, 5.13 % Cu, 3670 ppm Zn) however, the ore (Ch and M-t) used in experiments by Simpson et al., (2007) has significantly higher Cu, Zn, Pb and As. Based on this analysis, the dominant mineralogy of the ore used in the second report (Parry, 2008) is pyrite/marcasite and copper sulphides (chalcopyrite, covellite, digenite, bornite) with minor sphalerite/wurtzite and galena, whereas the ore used in the first study contains more zinc-sulphides (sphalerite/wurtzite), copper-sulphides and lead-sulphides. Gena, (2013) discusses the range of mineralogy and geochemistry within the Pacmanus hydrothermal system, where samples can be classified into

chalcopyrite-, sphalerite-, pyrite- or silica-rich ores. As the ore utilised in the EIS experiments was likely to be pyrite-rich based upon the metal concentrations the results can only claim to be applicable to one particular area in a deposit.

The EIS studies (Parry, 2008; Simpson et al., 2007) investigate a range of variables including grain size, geochemistry, time, fluid to rock ratio and temperature. Data from the EIS are illustrated in Figure 3 and show the concentrations of Fe, Cu, Pb, Zn, As, Ni, Mn, Al, Co and Cd released as a function of time. Raw data can be observed in Appendix B.

Both studies (Parry, 2008; Rzepka et al., 2014; Simpson et al., 2007) show that metal release can and does occur during oxidation of mixed sulphide ore in seawater at neutral pH. Both studies also show that the mineralogy and geochemistry play a large role in leaching rate, with Ulveryggen and Nussir tailings showing different leaching rates over longer periods (>30 days) and the EIS studies showing a major disparity in metals (and their concentrations) released with ore type. Copper concentrations reached 25 ppb after 100 days in Norway experiments, with the rate of leaching leveling off towards the end (70-100 days) of experiments. This is in comparison to a release of up to 500 ppb Cu shown over the EIS studies. The seafloor sulphide ore used in EIS experiments shows significant leaching of not only Cu but also other metals including Fe, Pb, Zn, As, Ni, Mn, Al, Co and Cd. Trace elements including As, Se, Ni, Zn and Pb were not shown to be leaching in Norway experiments, although detection limits of these elements were not provided.

When comparing sulphide ore type, Zn, Ni and Co released in Parry (2008)'s study is more significant in comparison to the ore(s) used in experiments by Simpson et al. (2007) that show higher release of Fe, Mn and Al although show comparable release of Pb and Cu to Parry (2008). The results are somewhat confusing when the metals released are compared to the initital ore chemistry. Experiments by Parry (2008) show significantly higher release of Zn, Ni and Co, and lower release of Fe and Mn. Whilst this is justified by the higher Co and Ni levels in the ore (Table 4), the initial chemistry indicates a much lower Zn concentration in the ore

in comparison to the higher concentrations in samples used by Simpson et al. (2007), which show a lower Zn release. Furthermore, with such a high Fe and Mn initial chemistry in Parry (2008)'s ore, the reason behind the lower release of these is unclear. Heterogeneity of the ores used is significant in this case, where the mineralogy could be varying across a micron scale but has simply not been documented. Interesting to note is the high concentrations of As in all samples with the exception of C-c (>2000ppm), yet the fairly low levels of As (<10ppb) that have leached. The formation of oxides and the absorption of trace metals such as As could be playing a role in this instance. Grain size, rock to fluid ratio and temperature were all shown to have an effect upon leaching of metals from sulphide ore. An increase in temperature and rock to fluid ratio (total suspended solids) were shown to increase the metal release whereas no linear relationship between particle size and metal release was found.

Rzepka et al. (2014) postulate an initial rapid dissolution of secondary copper minerals (corresponding to an initial tailings disposal) followed by a slower long-term surface leaching (after tailings have settled on the bottom). The slow leaching rate observed in these experiments was attributed to saturation conditions of sediments prohibiting supply of oxygen through the tailings (Rzepka et al., 2014). The saturation conditions of sediments in this scenario may be valid, but are ultimately a function of grain size (which is not provided) and subsequent pore space and permeability. When comparing this to the deep-sea mining of SMS deposits, whilst this may be comparable to the dewatering stage of the mining process (albeit with a different mineralogy/geochemistry), it is ultimately very different to the extraction phase which will result in a higher surface area of material exposed to oxidation for longer lengths of time.

4 Galvanic coupling

Seafloor sulphide ore deposits very rarely contain only one individual sulphide mineral. The majority of deposits contain a mixture of sulphide minerals in different abundances that can include pyrite, marcasite, pyrrhotite, chalcopyrite, isocubanite, sphalerite/wurtzite, galena, secondary Cu sulphides (bornite, covellite, digenite, chalcocite) and sulphosalts (tennantite-tetrahedrite amongst many

others) as well as numerous other minerals in only trace amounts that are not considered further.

Galvanic interactions have never been fully considered in this context of oxidative dissolution of a natural SMS ore deposit. A galvanic cell occurs where two different sulphide minerals are in physical contact. The mineral with the lower resting potential behaves as an anode and preferentially dissolves, protecting the other mineral which is behaving as a cathode (Mehta and Murr, 1983). This is shown schematically in Figure 1. As highlighted by Heidel et al. (2013), when in contact with other sulphides, pyrite should be galvanically protected as a result of its high rest potential (E = 0.62-0.66 V) (Biegler and Swift, 1979; Mehta and Murr, 1983). This is in comparison to lower rest potentials observed for other sulphides, with a review of rest potentials of sulphide minerals at different pH shown in Table 3. Rest potentials quoted are relative to a Standard Hydrogen Electrode (SHE).

To a certain extent, the impact of galvanic coupling for mineral dissolution can be predicted based on the individual sulphide mineral rest potential given in Table 3. However, when there are multiple sulphide phases all in contact with one another, the resulting cells have the potential to be complex. Furthermore, the rest potential of sulphide minerals is a function of their host electrolyte, pH, temperature and their natural impurities. For instance, the rest potential of pyrite, pyrrhotite and galena are shown to vary as a function of pH (an increase of pH leading to a decrease in rest potential) (Sui et al., 1995).

Galvanic interactions have been reported in the literature (Abraitis et al., 2004a; Da Silva et al., 2003; Heidel et al., 2013; Koleini et al., 2010; Kwong et al., 2003; Li et al., 2006; Liu et al., 2008; Mehta and Murr, 1982), largely in the context of terrestrial sulphide ore deposits and their production of acid rock drainage.

Whilst not attributed to galvanic interactions, Edwards et al. (2003) clearly demonstrated that a mixed sulphide ore is more reactive on the seafloor than individual sulphide minerals (pyrite, marcasite, chalcopyrite, sphalerite) albeit in the presence of bacteria. Recently, precious metal-rich Fe-oxy-hydroxide

sediments have also been reported from a deposit in the Cayman Trough (Webber et al., 2015) and are thought to be influenced by galvanic reactions. Similarly, a study by Koski et al. (2008) examined a terrestrial VMS deposit in Prince William Sound, demonstrating a sequence of increasing resistance to oxidation in the order: pyrrhotite « sphalerite <chalcopyrite ≤ pyrite, (Ridley, 2012) but it is unknown if a similar sequence of reactivity applies to seafloor conditions.

Kwong et al. (2003) demonstrated the occurrence of galvanic sulphide oxidation in shallow water at a near-neutral pH within mine wastes that contain mixed sulphides and/or sulphosalts, and how this type of oxidation has the ability to enhance metal leaching. However, Sui et al. (1995) showed that specific rest potentials of sulphide minerals decrease with increasing pH, which would suggest they have less impact in a neutral pH seawater context. However, the relative difference in rest potential between the sulphides is fairly constant and it is this that dictates the effect of the galvanic cell.

Other similar galvanic leaching studies have been undertaken in a variety of media including chloride, sulphate and H_2SO_4 at a range of pH's and temperatures (Mehta and Murr, 1982; Sui et al., 1995; Kwong et al., 2003; P.K Abraitis, Pattrick, Kelsall, et al., 2004; Qing You et al., 2006; Li et al., 2006; Koleini et al., 2010; Majuste et al., 2012; Heidel et al., 2013). Whilst it is difficult to apply the results to a neutral pH, seawater context, they are still of significant importance. The presence of pyrite has been shown to increase the leaching of chalcopyrite across multiple studies using different media (Abraitis et al., 2004a; Koleini et al., 2010; Majuste et al., 2012; Mehta and Murr, 1982). Majuste et al. (2012) demonstrated that this galvanic effect is enhanced under less oxidising conditions. This could be of significance in certain hydrothermal environments where local seawater is not as oxygenated as atmospherically equilibrated surface waters. This could, for example, apply to the deepest part of the mid-ocean ridges or to isolated basins in back-arc settings.

Other studies investigate the effect Fe^{3+}, pH and flow rate of the electrolyte have in galvanic oxidation of sulphides (Li et al., 2006; Qing You et al., 2006), with greater

Fe^{3+} in solution and flow rate both shown to increase rate of galvanic interactions whilst increasing pH decreases galvanic potential but increases the overall reaction rate. Both studies indicate the significance of water currents and Fe^{3+} concentrations in the surrounding seafloor environment of an SMS deposit.

Heidel et al. (2013) undertook abiotic experiments with pyrite, galena and sphalerite mixtures at two pH conditions of 2 and 6 and concluded that results from single sulphide oxidation experiments cannot be used to derive results of oxidation of sulphide mixtures. During the 100 day experiments, pyrite was galvanically protected whilst galena and sphalerite behaved as anodes and were preferentially dissolved. They concluded that the variables that control oxidation rate of polymetallic sulphide ore deposits are: pH, the minerals present, Fe content of each mineral, abundance of minerals and mineral grain size (specific surface area). Weathering features of the sulphide minerals posterior to experiments suggested that galena is more reactive than sphalerite, which is in agreement with studies by Da Silva et al. (2003).

Galvanic interactions observed in experiments by Heidel et al. (2013) are in agreement with observations of preferential oxidation in natural clay samples from an abandoned polymetallic sulphide mine in Freiberg, Saxony, Germany (Tichomirowa et al., 2003). Both show the galvanic protection of pyrite and the preferential oxidation of both sphalerite and galena. Clay samples contained a high percentage of uncorroded pyrite, some galena grains with anglesite coatings and minimal residual sphalerite (suggesting near complete sphalerite oxidation).

Many other studies are related to sulphide ore processing including flotation where galvanic interactions are observed to be commonly occurring and result in increased oxidation (Chandra and Gerson, 2009; Dichmann and Finch, 2001; Ekmekçi and Demirel, 1997; Majima, 1969; Subrahmanyam and Forssberg, 1993; Sui et al., 1995; Yelloji Rao and Natarajan, 1989; Zhang et al., 1997). Majima (1969) shows how galvanic interactions were shown to increase oxidation, in particular for galena, sphalerite and covellite, which are oxidised 8 to 20 times faster when pyrite is present. It has also been suggested that the combination of

impurities within sulphides and galvanic couples have a significant impact on the flotation process (Chandra and Gerson, 2009).

5 Other variables

Other factors that impact sulphide mineral oxidation are important to assess. For example, in a neutral pH, bicarbonate buffered system, it has been shown that dissolution is largely controlled by initial particle size (Antonijević et al., 1997; Bouffard et al., 2006; Dimitrijevic et al., 1996; Feely et al., 1987; Long and Dixon, 2004; Wiersma and Rimstidt, 1984) and the available surface area (Arora et al., 1978; Avery and Benning, 2008, 2007; Bierens de Haan, 1991; Evangelou and Zhang, 1995; Gartman and Luther, 2014; Lasaga, 1981; McKibben and Barnes, 1986; Moses et al., 1987; Pugh et al., 1984; Wiersma and Rimstidt, 1984).

Most studies in the literature have observed or assumed that dissolution rate is linearly dependent upon surface area. However, as a result of "reactive surface area" (McKibben and Barnes, 1986), oxidation products as inhibitors (Bouffard et al., 2006; Huminicki and Rimstidt, 2009; Long and Dixon, 2004; Nicholson et al., 1988) and non-perfect cleaning of pyrite surfaces (Bierens de Haan, 1991; Clarke et al., 1995; Heidel et al., 2013; McKibben and Barnes, 1986; Moses et al., 1987; Parthasarathy et al., 2014; Wolfe et al., 2007), this has been difficult to prove. McKibben and Barnes (1986) found oxidation of pyrites was non-uniform with most oxidation occurring at sites of excessive surface energy, specifically along grain edges, corners, defects, solution pits, fluid inclusion pits, cleavages and fractures known as ‘reactive surface area’. Seafloor sulphide minerals can display a range of textures (massive, colloform, fambroidal) and grain size, which will ultimately dictate both reactive and total surface area. In one example, Wiersma and Rimstidt (1984) demonstrate how low temperature pyrite (early diagenetic) has a specific surface area an order of magnitude higher than that of their high temperature pyrite and marcasite.

Over time this oxidation on the surface becomes inhibited by the formation and build up of iron oxides, iron oxy-hydroxides and elemental sulphur that limits the contact and diffusion of oxygen to the surface (Bouffard et al., 2006; Huminicki and

Rimstidt, 2009; Long and Dixon, 2004; Nicholson et al., 1988), with passivation shown to occur at high pressure conditions (Long and Dixon, 2004). However one study by Gartman and Luther (2014) has shown that dissolution of sub-micron pyrite is fundamentally different (and slower) than that of larger particles where particle size and surface are not significant; whereas concentration of available reactants are. Furthermore, the formation of an iron oxide coating on the surface of the sub-micron particles appeared to have no impact on oxidation rate.

Solubility of oxidation products has been shown to play an important role in oxidation rates (Heidel et al., 2013). During abiotic oxidation experiments with a mixed sulphide (galena, sphalerite, pyrite), secondary weathering products of anglesite and elemental sulphur were observed on galena grains but did not appear to passivate galena until after day 50 (for pH 6 experiments) when lead concentrations were shown to decline. Sphalerite is shown to consistently oxidise throughout the early stages of dissolution in the presence of pyrite at pH 6, evidenced by increasing Zn concentrations throughout with concentrations remaining consistent or falling slightly after day 50.

Other important factors include Fe^{3+} (Antonijević et al., 1997; Dimitrijevic et al., 1996; McKibben and Barnes, 1986), Fe^{2+} (Garrels and Thompson, 1960; Moses and Herman, 1991; Rimstidt and Vaughan, 2003), impact of stirred/unstirred conditions (Chandra and Gerson, 2010; Holmes and Crundwell, 2000; Wiersma and Rimstidt, 1984), and Eh (which is correlated with dissolved oxygen (DO) and Fe^{3+}) (Chandra and Gerson, 2010; Williamson and Rimstidt, 1994). As discussed earlier, mixed sulphide minerals and the potential for galvanic coupling highlight the significance of electrochemical processes (Chandra and Gerson, 2010).

5.1 The role of microbes

One area that has been the subject of a great deal of research is related to how sulphide minerals provide energy to support chemolithoautotrophic microbial growth. The oxidation or dissolution of sulphide minerals within these ore deposits provides free energy that is then harnessed by organisms and provides a source of energy. It has been shown in the literature that microbes mediate sulphide

mineral dissolution (McGuire et al., 2001) and appear to increase the rate of dissolution (Fowler et al., 1999; Lizama and Suzuki, 1989).

It is widely accepted that Fe-oxidising bacteria play a significant role during the weathering (oxidative dissolution) of seafloor sulphide ore deposits (Edwards et al., 2003). Corkhill (2008), Koski et al. (2008), Plumlee et al. (1999) and Rimstidt et al. (1994), all suggest that redox reactions utilising Fe^{3+} (which is produced by bacteria) play a significant role in enhancing reaction rates of sphalerite, chalcopyrite, enargite and arsenopyrite. Thiobacillus ferroxidans and Thiobacillus thiooxidans have both been shown to increase the leaching of metals (Fe, Cu, Zn) from sulphide minerals (pyrite, chalcopyrite, sphalerite) by up to 44.2 % in some cases (Lizama and Suzuki, 1991). It has also been reported in numerous dissolution studies (Ahonen et al., 1985; Berry et al., 1978; Jyothi et al., 1989; Mehta and Murr, 1983, 1982, Natarajan, 1988, 1985, Natarajan and Iwasaki, 1983, 1986; Yelloji Rao and Natarajan, 1989) that the presence of bacteria such as Thiobacillus ferroxidans in a polymetallic sulphide mixture is known to accelerate galvanic interactions by several times. In one particular study, oxidation of sphalerite in the presence of bacteria was increased 30-fold when in a mixture with pyrite (Malouf and Prater, 1961). The combined impact of bio-leaching and galvanic interactions (between chalcopyrite and pyrite) was shown to increase the dissolution rate of copper by a factor of 8 with Thiobacillus ferroxidans at 10°C in comparison to a single chalcopyrite system (Mehta and Murr, 1983). The effect is so great that a bioleaching process using Thiobacillus ferroxidans has been developed and tested for use in the recovery of precious metals (Au, Ag) from terrestrial polymetallic sulphide ores and their tailings (Attia and El-Zeky, 1990).

Whilst the role of microbes is highly important in the longer-term, in-situ, natural oxidation of seafloor sulphide ore deposits, it has been suggested that abiotic oxidation rates of sulphide minerals are more relevant to the oxidation of sulphides during seafloor mining. It is postulated that bacterial colonization of freshly ground mineral surfaces is unlikely under the rapid time spans of mining (minutes to days) (McBeth et al., 2011).

6 Discussion

This review of the experimental literature illustrates the paucity of data that can realistically be applied to simulating the processes that might be important to economic factors in SMS prospecting, extraction and environmental impact. There are no studies that emulate the true range of composition of the sediments that will be dispersed into aqueous suspension as a result of deep-sea mining. This suspended material will include a variety of minerals, and it is the interaction of these minerals and crystal inclusions in regards to galvanic cells that have the ability to substantially increase the release of metals into the water column (Abraitis et al., 2004a; Heidel et al., 2013; Koleini et al., 2010; Kwong et al., 2003; Li et al., 2006; Liu et al., 2008; Majuste et al., 2012; Mehta and Murr, 1983; Subrahmanyam and Forssberg, 1993). There are a multitude of variables to consider in regards to such dissolution including mineralogy, bulk elemental chemistry, grain size distribution and surface area of the sediments as well as the temperature, pressure, salinity, pH, oxidising agents and seawater composition.

The only dissolution study that exists that emulates a true composition of sediments in seawater was undertaken as a result of prospecting and a regulatory need to provide an environmental impact statement for mining the Solwara 1 Deposit in Papua New Guinea (Gwyther, 2008a). This study was undertaken with three 'representative' sulphide ores, at conditions that are not realistic (higher temperature, 1 atm pressure). The sulphide ore utilised was not characterised in terms of mineralogy, therefore it is difficult to evaluate and for instance say whether galvanic cells could have been playing a role.

The following section aims to highlight the important variables for considerations in terms of undertaking future oxidative dissolution experiments that emulate both the natural and anthropogenically effected dissolution process of seafloor polymetallic sulphide ore deposits. This is the beginning of a roadmap for research that is essential to the efficient mining of SMS deposits.

6.1 Temperature

Sulphide oxidation rate will increase significantly with increasing temperature as it

influences the kinetics of the reaction (Chandra and Gerson, 2010, and references therein). This variable is dependent upon where in the world this natural weathering process and/or mining process is occurring. Deep sea temperatures are unlikely to be significantly different across the world (Atlantic 4km: 2°C; Bismarck Sea 1.5km: 3°C (Gwyther, 2008a)). If mining occurs on an inactive vent, at a distance from active vent fields, these average sea temperatures are likely to be representative for experiments on weathering. However, in terms of mining (extraction/dewatering), the depth at which any suspended material is located is likely to have a significant impact on dissolution in terms of temperature, with temperatures of 27-31°C at the sea surface of Bismarck Sea and around 10°C at 400 m depth (Gwyther, 2008b).

Exit temperatures of fluids from hydrothermal vents range from 60 to as high as 400°C (e.g. Haase et al. (2007). There is also the potential for a range of lower temperatures (<50°C) in regards to diffuse flow but this water is ultimately a mix of seawater and vent fluid rather than seawater (Le Bris et al., 2006; Rona and Trivett, 1992; Scheirer et al., 2006). However, any elevated seawater temperatures are generally restricted to within centimetres to metres of the temperature source (hydrothermal fluid/diffuse flow) (Johnson et al., 1988; Rona et al., 1984; Rona and Trivett, 1992), where entrainment of cold ambient seawater quickly reduces temperatures to background levels.

Furthermore, mining is unlikely to ever take place near any active venting due to hazardous conditions and limitations of operating capabilities of seafloor mining tools, with operating temperatures from 0 to 35° C outlined by Nautilus Minerals Inc (Gwyther, 2008b).

6.2 Pressure

There have been numerous studies that illustrate how high partial pressure of oxygen can promote faster sulphide dissolution (Chandra and Gerson, 2010; Karastelev, 2013; Koslides and Ciminelli, 1992; Long and Dixon, 2004; McDonald and Muir, 2007; Peters, 2010; Rusanen et al., 2013). However, at high partial pressures of oxygen, it has also been shown that passivation can occur more

readily, due to surfaces being filled with elemental sulphur (Chandra and Gerson, 2010; Long and Dixon, 2004). This has the potential to reduce dissolution rates considerably.

Hydrostatic pressure has been shown to have minimal effect on dissolution rates with individual minerals (Baldo, 1992) as there is no increase in partial pressure of oxygen. As well as this, seawater is an incompressible liquid with no significant increase of collisions of reactants expected. However, the effect hydrostatic pressure might have on galvanic coupling has not been investigated and this could have an impact on dissolution.

6.3 pH

pH of the waters in a mining environment is crucial at it has the ability to impact the sulphide oxidation rate (Acero et al., 2007; Bonnissel-Gissinger et al., 1998; Millero et al., 1987), with lower pH's increasing the oxidation rate (Chandra and Gerson, 2010, and references therein). Millero et al. (1987) showed that the rate increased by four times for a pH 4.0 in comparison to pH 8.0. It will also greatly impact the toxicity and reactivity of heavy metals, with the speciation and solubility of heavy metals dictated by pH. Furthermore, it has also been shown that the sensitivity to metals by organisms can be affected by pH (Ho et al., 1999; Wong and Yang, 1997). The presence of bacteria, their population numbers and species type, which ultimately impact the natural weathering process, is also influenced by pH.

pH of ambient seawaters across the world varies between 7.5 to 8.4, with a current average pH of 8.1 (Tanhua et al., 2015). Inactive hydrothermal vents are likely to experience this more neutral pH, depending on the time since activity and their proximity to active vents.

Hydrothermal fluids from black smokers, bottom seawaters around vents and diffusers on the MAR show a range of pH from 2.5 to 7.9 (Charlou et al., 1996; Desbruyères et al., 2001; Le Bris et al., 2001; Sarradin et al., 1999, 1998, Von Damm, 1995, 1988). While pH shows large variations during the turbulent mixing of these variable hydrothermal fluids and cold, ambient seawater, and can create

gradients (Haymon and Kastner, 1981; Le Bris et al., 2001), they are generally restricted to areas close to the active chimney surface or plume. pH measurements observed above hydrothermally active volcanoes of the Mariana Arc, Axial Volcano and Southern East Pacific Rise by Resing et al. (2004;2009) show a wide range of pH decrease above vent sites. However, changes are small and restricted to 10s of km of the active vent, with most pH decreases on the order of 0.1 pH unit from their regional backgrounds (Resing et al., 2009, 2004). pH will ultimately be site specific and is more likely to vary as a function of which ocean and depth mining is occurring at rather than distance from an active vent.

6.4 Oxygen concentration

The oxygen concentration is highly dependent on where the weathering and/or mining process is occurring. For example, the Atlantic Ocean has a much higher oxygen content (on average between 8-9 mg L^{-1}) than the Pacific Ocean (4-6 mg L^{-1}), but this varies dramatically from place to place (Schlitzer, 2000). The less oxygenated the environment, the lower the oxidation rate and the more limited oxidation and precipitation will be.

6.5 Seawater composition and Fe^{3+} as an oxidising agent

Seawater composition in terms of the proportions of the major constituents is fixed and constant across the world, however in terms of salinity - seawater is not uniform. If concentrations of potentially toxic elements (Cu, Zn, Co, Ni, As, Hg, Pb) are already present in the environment, it is possible that ecosystems are already adapted and therefore the risk is reduced. However, of most importance in this regard, are elements that can act as oxidising agents. Oxygen concentrations were discussed earlier, but other oxidising agents including Fe^{3+}, MnO_2 and nitrate NO_3^- are present in seawater. However, the dominant oxidising agent in an oxic environment is Fe^{3+} and it is a powerful oxidant in acidic environments (Nordstrom and Alpers, 1999). Fe^{3+} is a more effective oxidant than O_2, with primary dissolution of pyrite driven by initial oxidation of Fe^{2+} by O_2 to Fe^{3+} (Eq. 6), which drives forward sulphide oxidation (Baker and Banfield, 2003) in Eq. 7. If there is significant Fe^{3+} already present in the ambient seawater, there is the potential for greater oxidation of sulphides as the rate is no longer dependent on Eq. 6 to

produce Fe^{3+}.

Equation 6

$$14Fe2++3.5O2\ aq+\ 14H+ \longrightarrow 14Fe3++7H2O$$

Equation 7

$$FeS2+14Fe3++8H2O\ \ 15Fe2++2SO42-+16H+$$

Oxidation of Fe^{2+} is slow below pH 4 and may limit the rate of oxidative dissolution of sulphide ore deposits (Baker and Banfield, 2003). However, if close to an active vent, pH is likely to be more acidic, thus being able to stabilize more Fe^{3+} and ambient concentrations of Fe^{3+} are also likely to be higher.

6.6 Grain size and surface area

The Solwara Environmental Impact Study (EIS) identifies two points of plume formation and metal release: initial removal of overburden and return water from the dewatering process (Gwyther, 2008b). The EIS states that the grain size produced will be 80% <25 mm and 20% of smaller unknown size. It also states there is the potential for formation of grains <10 μm in size where the cutter teeth meet the rock. Return water plumes are expected to have particles <8 μm. The natural grain size and texture of the deposit will also have implications in plume formation and surface area available for metal release, with smaller grains remaining in suspension longer and having higher surface area; making them more susceptible to dissolution. Furthermore, a combination of factors including the natural size of sulphide minerals, the size of sulphide inclusions within other sulphides and the grain size produced throughout the mining process will play a large role in whether galvanic calls are still present and operating. In terms of the natural weathering process, the SMS grain size is crucial here, for similar reasons explained above.

6.7 Fluid to rock ratio

It is suggested that the relationship between fluid to rock (F:R) ratio and dissolution rate is linearly proportional, within this context of a fluid dominated system.

However, the fluid to rock ratio would differ depending on whether we are focusing upon the natural weathering (highest F:R), the extraction process (lowest F:R) or the dewatering process.

6.8 Variation in mineralogy and geochemistry of seafloor sulphide ore deposits

SMS deposits occur in a range of tectonic environments including mature volcanic hosted mid-ocean ridges and younger sediment rich rifts (with varying rates of spreading), hot spots and arc-related settings (arc volcanoes, rifted arc crust, back-arc spreading centres). The host rock lithology is ultimately dictated by these tectonic controls, with a range of host rock compositions occurring including predominantly mafic to ultra-mafic (basalt, gabbro, serpentinite) along mid-ocean ridges and more evolved compositions (dacite, rhyolite) in arc settings as well as sediments in oceanic and continental crust (Hannington et al., 2005). These volcanic and tectonic controls ultimately dictate the availability of major and minor elements of seafloor massive sulphide ore deposits. Superimposed on this, the minor element endowment is influenced by the temperature-dependent solubility of the elements in question (Monecke et al., 2016). Characterisation of this variation is required in order to further understand, and predict metal leaching and environmental risk where mining certain deposits may have more or less impact than others (Jamieson et al., 2015).

In terms of major economic element trends, metal content of SMS deposits varies dramatically with volcanic and tectonic setting. SMS deposits located on mid-ocean ridges vary as a function of host lithology. Monecke et al. (2016) document this variation with the most comprehensive database of geochemical analyses to date. Stated here are median base metal contents of their database. Sediment covered ridges and basalt-hosted ridges contain a combined Cu + Zn + Pb content of 1.5 wt% and 3.2 wt% respectively. By comparison, ultramafic hosted ridges demonstrate a 13.2 wt% combined Cu + Zn + Pb, significantly higher. SMS deposits associated with convergent plate margins and more evolved (acidic) volcanic host lithology generally demonstrate higher base metal contents (rifted arc crust: 11.1 wt%, back arc spreading centres: 16.1wt% combined Cu + Zn +

Pb), with the exception of those located on arc volcanoes (3.6 wt% combined Cu + Zn + Pb).

Common trends are observed in trace element concentrations of sulphides from different settings. Mafic to ultra-mafic host rock dominated mid-ocean ridges consistently demonstrate high concentrations of Cu, Fe, Co, Se, Ni, Mo and Te. In comparison, volcanic arcs and young back arc rifts where more evolved volcanic host rocks are dominant show high concentrations of Zn, Cd, Pb, As, Sb, Hg, Ba, Tl and Au (Hannington et al., 2010, 2005; Monecke et al., 2016). It is important to note that most heavy metals that are of economic value also have the potential to be toxic to ecosystems (see Section 2.2.1) at significant concentrations (Ando et al., 2002; Jeanthon and Prieur, 1990; Llanos et al., 2000; Nies, 1999; Vetriani et al., 2005); most prominent here are Cu, Pb, As, Cd, Sb and Hg, largely associated with arc-related settings. However, the high concentrations of major heavy metals (Cu, Zn, Pb) from ultra-mafic hosted ridges also suggest that they have the potential to cause toxicity during any future mining.

Temperature also plays a large role, with higher temperature Cu rich chimneys (~350°C) associated with high concentrations of Co, Se and Mo. Lower temperature fluids (~250°C) show an association with Cd, Pb, As, Sb and Ag. It is therefore of the upmost importance to systematically sample high and low temperature assemblages across deposits to provide a more representative picture of bulk compositions in terms of economic endowment and potential toxicity (Hannington et al., 2010; Monecke et al., 2016).

Based on the current (but limited) knowledge of oxidation rates of individual sulphides in seawater (not including galena, secondary Cu sulphides, sulfosalts), it seems likely that sites with ores that contain a high abundance of pyrrhotite and marcasite are likely to oxidise quicker. In terms of galvanic coupling, ores that contain an abundance of pyrrhotite, sphalerite, sulfosalts and/or galena in the presence of pyrite, chalcopyrite and/or marcasite have the potential to oxidise and release metals at a faster rate. Both suggest that these ore types would ultimately lose their economic worth quicker, and have more potential to release toxic metals

during mining. Ultimately, this potential is dictated by the toxic trace elements found in these more reactive minerals (see Section 6.8.1) and the subsequent oxidation potential if released. This trace chemistry is a function of the composition of vent fluids which is ultimately dictated by tectonic setting (back-arc basin vs ridge vs hot spot), host rock lithology, pH and temperature amongst others (Monecke et al., 2016).

In reality, mining will only occur where there is a high abundance of economically worthy sulphide minerals and their base metals including chalcopyrite, isocubanite, secondary Cu sulphides (Cu), sphalerite/wurtzite (Zn), galena (Pb) as well as high concentrations of precious metals. Within this, pyrite and/or marcasite will commonly be present. In such a case, galvanic coupling is expected to arise and lead to an increase in preferential dissolution and release of metals, if not adequately balanced by oxidation.

6.8.1 Trace impurities in common SMS minerals

A compilation of available trace data in sulphide minerals from SMS samples collected worldwide provides an assessment of toxicity and potential for release and is presented in Table 5. The compilation also highlights the gaps in our knowledge of trace chemistry in sulphides. Here, we discuss only significant concentrations in regards to specific sulphide minerals across SMS samples worldwide.

In terms of trace element content of the seafloor sulphide minerals likely to oxidise quickest based on oxidation rate alone (pyrrhotite, marcasite), data are limited. Only three studies have analysed SMS pyrrhotites, two involve pyrrhotites from the Juan de Fuca Ridge (Paradis et al., 1988; Tivey et al., 1999) and the second, those from Rainbow vent field on the Mid-Atlantic Ridge (Marques et al., 2006). Only certain elements have been analysed, with no measurements of Hg, Sb or Pb. Where analysed, pyrrhotites show similar concentrations of Cd (0-400 ppm), hundreds of ppm of Cu and hundreds to thousands of ppm of Zn. Pyrrhotites from the Rainbow vent field show high concentrations of Co (600-4000 ppm) and a range for Ni (100-1100 ppm), attributed to ultra-mafic host rocks. A range of As

concentrations (<300 – 750 ppm) in pyrrhotites are observed at the Endeavour Segment along the Juan de Fuca Ridge (Tivey et al., 1999).

Marcasites are often grouped with pyrites, so it is difficult to separate the geochemistry of the two. Only two trace studies of marcasite exist and no consistent trends are observed. Hannington et al. (1991) analysed marcasite concentrates from Axial Seamount (hot spot and mid-ocean ridge) and observed significant concentrations of As (783-928 ppm). Marcasites from Alice Spring Field, Mariana Trough displayed significant concentrations of Zn (800 ppm).

Pyrites are observed to have slower oxidation rates in seawater in comparison to other sulphide minerals, and are often galvanically protected when in a cell with another sulphide mineral (due to its high rest potential). Pyrites from all settings can be observed to contain significant Cu and Zn as trace impurities, and those from arc related settings can show high concentrations of Pb and As (hundreds to thousands of ppm). Cobalt and nickel is observed to be high in pyrites from mid-ocean ridges that are ultra-mafic hosted including Rainbow vent field, MAR and Kairei vent field, Indian Ridge (Marques et al., 2006; Wang et al., 2014).

Oxidation rates of sphalerite in seawater are limited to one study, but indicate a quicker oxidation rate than pyrite and chalcopyrite. Galvanically, sphalerite would be anodically dissolved when in a cell with pyrite, marcasite or chalcopyrite, but protected if present with secondary Cu sulphides and/or galena. Seafloor sphalerites are consistently shown to contain high concentrations of Cd (hundreds to thousands of ppm). Sphalerites associated with arc-related settings generally show concentrations of As (1000-10000s ppm), Pb (1000-10000s ppm) and Sb (100-1000s ppm) much higher than that of ridge settings (10-100s ppm). Data for certain minor elements in sphalerite are lacking including Hg, Sn, Se, Ni, Mo along with critical metals (Te, Ga, Ge, In).

Trace data for galena in SMS deposits is limited to six seafloor hydrothermal regions globally (Iwaida and Ueno, 2005; Petersen et al., 2014, 2004; Suzuki et al., 2008; Tivey et al., 1999; Ueno et al., 2003). Concentrations of Sb and Ag are

shown to be consistently high across all sites, with the highest concentrations observed at arc-related settings. Limited data for Cd and Zn indicate the potential for high concentrations in galena (800-1100 ppm Cd and thousands of ppm Zn from Palinuro Volcanic Complex, Hook Ridge and the Endeavour Segment along the Juan de Fuca Ridge (Petersen et al., 2014, 2004; Tivey et al., 1999)).

Sulphosalts are an extensive group of complex sulphide minerals with the general formula $A_mB_nS_p$ where A is a metal (Cu, Pb, Ag, Fe, Hg, Zn) and B is a metal or semi-metal (As,Sb,Bi, Sn). Sulphosalts are generally observed in arc-related settings with enargite (Cu_3AsS_4) and the tennantite-tetrahedrite solid solution series ($Cu_{12}As_4S_{13}$-$Cu_{12}Sb_4S_{13}$) most common. There is little known on the galvanic potential of sulphosalts, however, they are shown to oxidise quicker than other sulphide minerals (Fullston et al., 1999). Sulphosalts are a large sink for As, Sb, Pb and Cu, and therefore have high potential to be toxic during oxidative dissolution.

Both sulphosalts are consistently shown to contain significant concentrations of Ag (thousands of ppm) (Binns and Scott, 1993; Halbach et al., 1993; Petersen et al., 2014, 2004; Suzuki et al., 2008; Ueno et al., 2003; Watanabe and Hayashi, 2014; Wohlgemuth-Ueberwasser et al., 2015). Zn and Fe concentrations within both enargites and tennantite-tetrahedrite are significant (thousands to tends of thousands of ppm).

Hg data are only available at two sites: Palinuro Volcanic Complex and Hook Ridge, but demonstrate that Hg has a large affinity for sulphosalt phases over all other sulphide minerals (hundreds to thousands of ppm). High Se concentrations in sulphosalts are observed at Hook Ridge (900-1000 ppm) but this is inconsistent across all SMS deposits (Petersen et al., 2004; Wohlgemuth-Ueberwasser et al., 2015). Where data for Pb in tennantite-tetrahedrite are available, Pb is consistently high (thousands of ppm) across Palinuro Volcanic Complex, Hook Ridge, Okinawa Trough and Pacmanus (Binns and Scott, 1993; Ueno et al., 2003; Petersen et al., 2004; Petersen et al., 2014; Wohlgemuth-Ueberwasser et al., 2015). Data for Bi, Co and Ni (amongst many other economic metals (Ga, Ge, In, Sn, Tl) for

tennantite-tetrahedrite and enargite) in any SMS deposit are not observed in the published literature.

Secondary copper sulphides (bornite, covellite, chalcocite, digenite) are shown to oxidise quicker than other common sulphide minerals (Fullston et al., 1999) and are shown to have relatively low rest potentials (only higher than galena). Trace data for secondary copper sulphides in SMS studies are limited to six studies across six different sites and vary considerably. High average concentrations of Ag are observed at Pacmanus Chimney (bornite), Hook Ridge (covellite), Menez Gwen Field (covellite) and Carlsberg Ridge (bornite/digenite) with 1700, 1050, 588 and 230-350 ppm respectively, although this is not consistent with an average of <200 ppm of Ag observed in covellite at Kairei vent field, Indian Ridge. Se concentrations can be significant in secondary Cu sulphides from ultra-mafic hosted sites (chalcocites from Logatchev (87.9 ppm), with covellites from Kairei vent field also showing enrichment (250 ppm Se). However, this is contradictory to bornites and digenites from Wocan hydrothermal field along Carlsberg Ridge, where Se concentrations are <1.5 ppm. There are no trace data available for Bi, Ga, Ge, Mo, Sn and Tl for chalcocite and covellite and no trace data for Cd, Co, Hg, Ni and Pb for chalcocite.

Chalcopyrites are shown to have slower oxidation rates in seawater in comparison to other sulphide minerals, and have a high rest potential, indicating that they are unlikely to anodically dissolve (unless in contact with only pyrite/marcasite). Trace elements in chalcopyrites are shown to vary considerably from site to site, with some essentially ‘barren’ and others showing significant minor element endowment. The only consistent trend amongst all chalcopyrites analysed from all sites is the significant presence of Zn (on average: thousands of ppm). Concentrations of As are fairly low (tens of ppm) in chalcopyrites from ridge settings whilst those from Pacmanus Basin, Satanic Mills in particular, are significantly higher (12326-15714 ppm) (Binns and Scott, 1993; Wohlgemuth-Ueberwasser et al., 2015). Co and Ni concentrations in chalcopyrite are observed to be anomalously high at Rainbow vent field (thousands of ppm), related to the ultra-mafic host lithology. Pb and Sb in chalcopyrites from arc settings are generally high (hundreds of ppm). Concentrations of Se are high (190-640 ppm) at

ridge settings (TAG, Southern Explorer Ridge, Turtle Pits, Logatchev). Data for Ga, Ge, In, Sn, Tl in chalcopyrites from SMS deposits is limited to one hydrothermal field studied by Wang et al. (2017).

Isocubanite ($CuFe_2S_3$) is a cubic polymorph of cubanite and characteristic of high temperature seafloor sulphide mineral assemblages. Trace element data in isocubanites from SMS deposits are limited to four sites across four studies. Zn concentrations are consistently high across all four sites, with averages ranging from 1550 to 7100 ppm. Data for Co and Ni are limited to only two sites (Kairei and Rainbow), with Co concentrations consistently high ranging from 700-5200 ppm and variable to high Ni (700 ppm) at Rainbow, attributed to the ultramafic host rock at both sites. Se concentrations are limited to Kairei only, but shown to be significant (1400 to 2000 ppm). There are no published data available for Bi, Ga, Ge, Hg, In, Mo, Sn, Tl in isocubanites from SMS deposits.

There is often a distinct association between the texture of sulphide minerals and their trace chemistry, where colloform and porous phases are commonly observed to contain higher concentrations of certain traces (Lein et al., 2010; Wohlgemuth-Ueberwasser et al., 2015). However, it is clear that this trend is not always consistent across sites, minerals and/or elements, which is likely to be a result of varied initial trace impurity and subsequent site and mineral specific recrystalllisation.

6.9 Time

There has been no study to determine the time it takes for a seafloor deposit to ultimately be destroyed by physical and chemical weathering. This information would be critical if there is to be serious consideration of exploiting deposits associated with inactive vents, as it would help ascertain the cut off point for viability in terms of exploration - at least in regards to mid ocean ridges where crust is sequentially younger towards the ridge axis. Deposits where gossans are observed are a good indicator in terms of the rate of weathering. U-Th dating was used by Lalou et al. (1990) to determine that the currently active sulphide deposit of TAG, Mid Atlantic Ridge started forming 40 to 50,000 years ago, and provide a maximum time the deposit has been exposed to seawater. This provides an

indication that deposits of this age still have the potential to be of economic worth.

On the shorter timescale and to fully understand the concentration of metals that have the potential to be released over time during mining, it is necessary to know for how long the extraction and dewatering process will occur for any one particular time frame. The Solwara EIS states that it will take approximately 6 minutes to take the return water from the surface to the point of discharge above the seafloor (Gwyther, 2008b). Ultimately, the overall mass of return water that will be pumped to the seafloor is crucial to know here. The EIS states that ore will typically be extracted at a rate of 5,900 tonnes per day, and will take place no longer than 20 hours a day. As a result of the heterogeneity of the mineralogy and geochemistry in one deposit, the release of metals is unlikely to be consistent over time.

7 Direction for new research

This review paper brings together lines of evidence from a range of literature sources including those with a focus on both terrestrial and seafloor sulphide ore deposits, the mining process (extraction and flotation) and those dealing with acid rock drainage. It demonstrates our limited understanding of dissolution processes for a realistic mixed hydrothermal sulphide ore on the seafloor and highlights the questions that require answers going forward. Based on the literature presented here, different sulphide ore deposits will be oxidising and releasing a variety of different metals, all at different rates. Galvanic cells have never been fully considered in this context, and as demonstrated have the ability to increase dissolution rates of sulphides significantly. If heavy metal release is not temporally balanced by precipitation of oxide phases, there is the potential for ore deposits to gradually lose economic worth.

The factors that are likely to impact this process have been highlighted here, but no studies emulate the true range of mineralogies and geochemistries for these deposits that are naturally dissolving in a colder, deeper (high P), more saline, neutral pH environment. Furthermore, with an ever-increasing focus on mining

deposits associated with hydrothermal vents (both active and inactive), it is crucial for us to understand how this process is impacting the economic worth of deposits as they age and if this dissolution process can inadvertently be increased anthropogenically through mining. If so, subsequent heavy metal release (unbalanced by oxide precipitation) may have environmental implications including bioaccumulation in local (potentially exotic) ecosystems and dispersal or accumulation in the wider ocean.

As a result of the significance of temperature and pH upon the oxidation of sulphides, we suggest that mining inactive deposits - deposits that are not in proximity to higher temperatures and lower pH's - are likely to be comparably more 'eco-friendly' than mining active counterparts (assuming a like-for-like comparison) in terms of dissolution and metal release. Certain sites will be more predisposed to oxidation as a result of their mineralogy and geochemistry (those containing major pyrrhotite, marcasite, galena and secondary copper sulphides) and/or environment (higher temperatures, oxygen concentrations and lower pH's). Furthermore, certain sites pose more of an environmental risk (in terms of toxicity) than others, with arc-related SMS deposits associated with higher concentrations of As, Pb, Sb, Cd and Hg and ultra-mafic hosted SMS deposits associated with high concentrations of Co and Ni. Whilst studies on galvanic cells, individual mineral oxidation rates in seawater and leaching of certain polymetallic sulphides can give some indication, a broader study of oxidative dissolution with a variety of natural SMS ore deposits in seawater at correct conditions can provide a more realistic picture. This type of study can predict which sites (ore type, tectonic setting, environment), should be monitored more closely in regards to both reduction of economic worth over time and environmental impact if mining takes place.

Table 1 Characteristics of a range of seafloor Fe oxide/oxy-hydroxide deposits.

Type of Fe oxide/ oxy-hydroxide deposit	Mineralogy	Formation Process	Distinguishing Characteristics	References
Gossan	Trace sulphide minerals (pyrite, chalcopyrite, sphalerite) Secondary Cu sulphide minerals (covellite, digenite, chalcocite) Weathering products of sulphides (jarosite, atacamite) Fe oxides Fe oxy-hydroxides	Oxidation of a seafloor sulphide ore chimney or mound shaped deposit.	Small in size (representing weathered sulphide chimneys) Frequently located along ridge axis where sulphide rich fluids still dominate or have dominated in the past	Hannington et al. (1988) Herzig et al. (1991) Hannington (1993)
Ochre	Fe oxides Fe oxy-hydroxides Smectite/clays Fe-Mn crusts	Primary oxides and oxy-hydroxides formed through slow exhalative venting.	Cover large areas (>200m in diameter) Located on off-axis seamounts and intra-plate edifices	Hekinian (2014)
Primary precipitates	40-80% $Fe_2O_3.H_2O$	Primary precipitates formed through hydrothermal alteration or through alteration reactions between hot lava flows and seawater.	Do not contain any secondary sulphide minerals Do not contain high clay content Low transitional metal contents Low SiO2 and sulphur Higher degree of iron oxidation	Hekinian (2014)
Plume fallout sediments	Fe oxides Fe oxy-hydroxides	Primary oxides in the hydrothermally derived plume precipitate and settle	Proximal or distal to chimney or hydrothermal plume	Dymond and Roth (1988) Feely et al. (1990) Hannington and Jonasson (1992) Goulding et al. (1998)

Table 2 Published and calculated oxidation rates of sulphide minerals in seawater from both field and laboratory based experiments (Bilenker, 2011; Feely et al., 1987; Morse, 1991; Romano, 2012). Rates are determined at a variety of conditions including salinity, pH, temperature, partial pressure of oxygen, hydrostatic pressure and grain size/surface area.

Sulphide Mineral	Formula	Study	Field/Lab	Method	Source	S (‰)	pH	T (°C)	P_{O2} (atm)	Pressure (bars)	Grain size (μm)	SA (cm^2)	Oxidation Rate			
													mol/kg/sec	Error +/-	cm/sec	Error +/-
Pyrite	FeS_2	Feely et al. (1987)	[1] Field	Mass change of sulphide over time	Black smoker particulates, Juan de Fuca Ridge	~35	7.5-8.4	1.8	n/a	220	1000-3000	n/a			5.30E-12	
		Feely et al. (1987)	[1] Field	Mass change of sulphide over time	Black smoker particulates, Juan de Fuca Ridge	~35	7.5-8.4	1.8	n/a	220	1000-3000	n/a			1.10E-11	
		Feely et al. (1987)	Lab	Solution analysis of Fe	Black smoker particulates, Juan de Fuca Ridge	n/a	8.3-8.6	25	1	1	20-53	n/a			6.70E-11	2.90E-11
		Morse (1991)	Lab	Solution analysis of pyrite	Hog Island, Galveston Bay, Texas (35 wt% <63um and 0.35 wt% organic C)	10	7.5-8.4	22	n/a	1	<62	n/a	[2] 2.00E-08		[3] 6.32E-09	
		Morse (1991)	Lab	Solution analysis of pyrite	Houston Ship Channel, Galveston Bay, Texas (5 wt% <63um and 0.05 wt% organic C)	10	7.5-8.4	22	n/a	1	<62	n/a	[2] 3.00E-08		[3] 9.48E-09	
		Morse (1991)	Lab	Solution analysis of pyrite	Houston Ship Channel, Galveston Bay, Texas (79 wt% <63um and 0.67 wt% organic C)	10	7.5-8.4	22	n/a	1	<62	n/a	[2] 6.00E-09		[3] 1.90E-09	
		Morse (1991)	Lab	Solution analysis of pyrite	Texas Shelf, 100m water depth	34	7.5-8.4	22	n/a	1	<62	n/a	[2] 5.00E-10		[3] 1.58E-10	
Marcasite	FeS_2	Feely et al. (1987)	[1] Field	Mass change of sulphide over time	Black smoker particulates, Juan de Fuca Ridge	~35	7.5-8.4	1.8	n/a	220	1000-3000	n/a			5.10E-11	
		Feely et al. (1987)	Lab	Solution analysis of Fe	Black smoker particulates, Juan de Fuca Ridge	n/a	8.3-8.6	25	1	1	20-53	n/a			2.50E-10	1.00E-10
Pyrrhotite	$Fe_{(1-x)}S$	Feely et al. (1987)	[1] Field	Mass change of sulphide over time	Black smoker particulates, Juan de Fuca Ridge	~35	7.5-8.4	1.8	n/a	220	1000-3000	n/a			1.10E-10	
		Romano	Lab	Solution	Dal N'gorsk Primorsky Kray	~35	3.15	19.5-	0.995	1	45-106	1190	[4] 4.25E-10	4.79E-	[5] 7.60E-	

[1] Mooring on southern Juan de Fuca Ridge, water depth 2205m.

[2] Calculated a rate from raw data (Appendix A) provided by Morse (1991) and applying a second-order polynomial fit in the form $y = y_0 + ax + bx^2$, where a is the initial rate given in mol/kg/sec (Bilenker, 2011; Romano, 2012)

[3] Calculated using method above (Appendix A) and using weight provided by Morse (1991), Mr of pyrite (118.98), density of pyrite (5.02 g/cm^3) and an average surface area of pyrite of 0.3 m^2/g (derived from the literature (Pugh et al., 1981; Wiersma and Rimstidt, 1984; Wolfe et al., 2007)).

[4] An average of experiments at similar run conditions (Bilenker, 2011; Romano, 2012).

Sulphide Mineral	Formula	Study	Field/Lab	Method	Source	S (‰)	pH	T (°C)	P_{O2} (atm)	Pressure (bars)	Grain size (μm)	SA (cm^2)	Oxidation Rate			
													mol/kg/sec	Error +/-	cm/sec	Error +/-
		(2012)		analysis of Fe	Mine, Far Eastern Region, Russia			20						11	12	
		Romano (2012)	Lab	Solution analysis of Fe	Dal N'gorsk Primorsky Kray Mine, Far Eastern Region, Russia	~35	3	34-35	0.995	1	106-150	330	[4]6.18E-10	2.72E-11	[5]3.98E-11	
		Romano (2012)	Lab	Solution analysis of Fe	Dal N'gorsk Primorsky Kray Mine, Far Eastern Region, Russia	~35	3	4	0.995	1	106-150	330	[4]1.30E-10	8.51E-12	[5]8.38E-12	
		Romano (2012)	Lab	Solution analysis of Fe	Dal N'gorsk Primorsky Kray Mine, Far Eastern Region, Russia	~35	2-4	21-22	0.995	1	106-150	330	[4]1.85E-10	2.41E-11	[5]1.19E-11	
		Romano (2012)	Lab	Solution analysis of Fe	Dal N'gorsk Primorsky Kray Mine, Far Eastern Region, Russia	~35	3	21-22	0.1	1	106-150	330	[4]1.82E-10	1.86E-11	[5]1.17E-11	
		Romano (2012)	Lab	Solution analysis of Fe	Dal N'gorsk Primorsky Kray Mine, Far Eastern Region, Russia	~35	3-3.5	21-23	0.01	1	106-150	330	[4]5.72E-11	3.68E-12	[5]3.68E-12	
Chalcopyrite	$CuFeS_2$	Feely et al. (1987)	[1] Field	Mass change of sulphide over time	Black smoker particulates, Juan de Fuca Ridge	~35	7.5-8.4	1.8	n/a	220	1000-3000	n/a			1.20E-12	
		Bilenker (2011)	Lab	Solution analysis of Cu	Casapalca Mine, Peru	~35	3	8.5-9.5	0.995	1	45-106	1273.4	[4]2.18E-12	1.90E-13	[5]4.62E-14	
		Bilenker (2011)	Lab	Solution analysis of Cu	Casapalca Mine, Peru	~35	3	21	0.1	1	45-106	1309.2	[4]2.54E-12	2.32E-13	[5]5.06E-14	
		Bilenker (2011)	Lab	Solution analysis of Cu	Casapalca Mine, Peru	~35	8.2	23.5	0.1	1	45-106	1376.45	[4]-3.92E-13	2.66E-13	[5]-7.32E-15	
		Bilenker (2011)	Lab	Solution analysis of Cu	Casapalca Mine, Peru	~35	4-4.5	22-23	0.995	1	45-106	1391	[4]7.94E-13	6.65E-13	[5]1.64E-14	
		Bilenker (2011)	Lab	Solution analysis of Cu	Casapalca Mine, Peru	~35	2-3	21-23.5	0.995	1	45-106	1394.94	[4]4.16E-12	3.13E-13	[5]8.09E-14	
Sphalerite	ZnS	Feely et al. (1987)	[1] Field	Mass change of sulphide over time	Black smoker particulates, Juan de Fuca Ridge	~35	7.5-8.4	1.8	n/a	220	1000-3000	n/a			2.40E-11	

[5] Calculated using raw data of Bilenker (2011) and Romano (2012), calculations presented in Appendix A.

Table 3 Rest potential of common sulphide minerals at ambient temperature.

Mineral	Formula	Origin	Solution or pH	Rest Potential (V) vs. SHE				Reference
					Bubbled with N2	Bubbled with O2	Exposure to air	
Pyrite	FeS_2	Unknown	1 M H_2SO_4	0.63			-	Majima (1969)
		Unknown	1 M $HClO_4$	0.62			-	Peters and Majima (1968)
		Unknown	4	0.66			-	Majima (1969) and references therein
		Huanzala, Peru	Distilled water, ~pH 7		0.405	0.445	0.485	Pozzo and Iwasaki (1989)
		Coahuila, New Mexico	0.001 mol/L Na_2SO_4		0.389	0.391	0.393	Hu et al. (2010) and references therein
Marcasite	FeS_2	Unknown	4	0.63			-	Majima (1969) and references therein
Arsenopyrite		Unknown	Distilled water, ~pH 7		0.277	0.303	0.323	Iwasaki (1989)
Pyrrhotite	$Fe_{(1-x)}S$	Unknown	1 M H_2SO_4	-0.28			-	Kovylina (1956)
		Sudbury, Ontario	Distilled water, ~pH 7		0.055	0.160	0.173	Adam et al. (1984)
		Stratheona Mine, Ontario	Distilled water, ~pH 7		0.125	0.262	0.295	Iwasaki (1989)
		Stratheona Mine, Ontario	Distilled water, ~pH 7		0.155	0.290	0.335	Hu et al. (2010) and references therein
		Stratheona Mine, Ontario	0.001 mol/L Na_2SO_4		0.262	0.277	0.308	Nakazawa and Iwasaki (1986)
		Stratheona Mine, Ontario	0.05 mol/L Na_2SO_4		0.058	-	0.190	Hu et al. (2010) and references therein
		Sudbury, Ontario	0.5 mol/L NaCl		-	0.071	-	Adam et al. (1984)
Chalcopyrite	$CuFeS_2$	Unknown	4	0.56			-	Majima (1969) and references therein
		Unknown	1 M H_2SO_4	0.52			-	Warren (1978)
		Unknown	1 M $HClO_4$	0.53			-	Majima (1969)
		Rouyn, Quebec	Distilled water, ~pH 7		0.190	0.355	0.371	Hu et al. (2010) and references therein
		Messina, S. Africa	0.05 mol/L Na_2SO_4		0.115	-	0.265	Hu et al. (2010) and references therein
Covellite	CuS	Unknown	4	0.45			-	Majima (1969) and references therein
		Unknown	1 M $HClO_4$	0.42			-	Majima (1969)
Chalcocite	Cu_2S	Unknown	1 M H_2SO_4	0.44			-	Kovylina (1956)
Bornite	Cu_5FeS_4	Unknown	4	0.42			-	Majima (1969) and references therein
Sphalerite	ZnS	Unknown	4	0.46			-	Majima (1969) and references therein
		Unknown	1 M H_2SO_4	-0.24				Kovylina (1956)
		Unknown	2	0.372				Da Silva et al. (2003)
		Unknown	0.5 mol/l NaCl, ~pH 10.5		0.030	-	0.060	Yelloji Rao and Natarajan (1989)
Galena	PbS	Unknown	4	0.4				Majima (1969) and references therein
		Unknown	2	0.325				Da Silva et al. (2003)
		Unknown	1 M H_2SO_4	0.28				Kovylina (1956)
		Brushy Creek, Missouri	Distilled water, ~pH 7		0.142	0.172	0.218	Learmont and Iwasaki (1984)
		Unknown	0.5 mol/l NaCl, ~pH 10.5		0.045	-	0.095	Yelloji Rao and Natarajan (1989)

Table 4 Metal concentrations in Nautilus ore samples utilised for dissolution experiments in reports by Parry (2008) and Simpson et al. (2007). Preparation and method of analysis was aqua regia digestion and subsequent ICP-OES for samples used by Simpson et al. (2007), method of analysis was not documented in the report by Parry (2008).

Study	Sample	Ag ppm	Al ppm	As ppm	Cd ppm	Co ppm	Cr ppm	Cu %	Fe %	Hg ppm	Mn ppm	Mo ppm	Ni ppm	Pb ppm	S %	Se ppm	U ppm	V ppm	Zn %
Simpson et al. (2007)	Ch-A-c	182	262	8420	580	59.3	1.3	10.4	1.81	-	126	-	3.3	9570	-	-	-	-	7.67
Simpson et al. (2007)	Ch-I-c	147	150	3930	291	440	0.7	0.136	4.98	-	653	-	4.8	4970	-	-	-	-	4.23
Simpson et al. (2007)	C-c	<0.5	1790	112	<0.3	19.8	3.6	0.0256	2.86	-	41.1	-	7.8	14.3	-	-	-	-	0.004
Simpson et al. (2007)	M-t	83	415	2370	172	61.7	1.3	2.67	10.8	-	383	-	4.2	1480	-	-	-	-	2.8
Parry (2008)	Solwara 1 ore	22.8	4000	1960.0	19.05	243.0	8.0	5.13	31.6	3.2	92.0	144.5	11.4	490.0	>10.0	138.0	10.1	29.0	0.367

Ch: Chimney, A: Active, I: Inactive, M: Sediment, c: used in elutriate experiments, t: used in toxicity experiments

Table 5 Trace element contents (ppm) of common sulphide minerals from SMS deposits derived from electron microprobe analysis (EPMA), laser ablation inductively coupled mass spectrometry (LA-ICPMS) and bulk analysis of mineral concentrates. *Abbreviations used:* MAR, Mid Atlantic Ridge; EPR, East Pacific Rise; JDFR, Juan de Fuca Ridge; PNG, Papua New Guinea.

No.	Ag	As	Cd	Co	Cu	Pb	Sb	Zn	Other	Location (setting)	Authors
Pyrrhotite ($Fe_{(1-x)}S$)											
27	200		200-300	600-4000	200			200-1900	100-1100 Ni	Rainbow vent field, MAR	Marques et al. (2006)
	400 -700		0-400		100-600			0-700		Southern JDFR	Paradis et al. (1988)
14	<400	<300 – 750			650			<600 - 800	<300 Se	Endeavour Segment, JDFR	Tivey et al. (1999)
Marcasite (FeS_2)											
2		783-928	137-154	60-200			40-74			Axial Seamount, JDFR	Hannington et al. (1991)
			0	0	100			800	100 Ni	Alice Spring Field, Mariana Trough	Iwaida and Ueno (2005)
Pyrite/Marcasite (FeS_2)											
22	0.31-412	41-2200	0-79	2.88-666.26	76-38000	7.4-6400	0.48-255.21	4-48090	0.5-157.7 Ni 0.003-668.15 Tl	Menez Gwen Field, MAR	Lein et al. (2010)
161		600		<200	<200		<200	<200	Max 600 Hg, Avg <200	Hook Ridge, Antarctica	Petersen et al. (2004)
85	<400	750-1676		<400	<700 – 2570	<1200	<100	<600 - 750	<400 – 3900 Mn	Endeavour Segment, JDFR	Tivey et al. (1999)
20		bdl-7200			bdl-2000			1550-8477	Avg 6333 Mn	Mothra hydrothermal field, JDFR	Kristall et al. (2006)
Pyrite (FeS_2)											
1	62	115	<10	51			5		124 Mo	TAG hydrothermal field, MAR	Hannington et al. (1991)
167	<400	<400		<400 – 1460	<600 - 2686	<1200 – 7075		<600 - 8783	<300 – 430 Se	TAG hydrothermal field, MAR	Tivey et al. (1995)
4	14-95	436-1740	<10-10	2-85			4-19		47-62 Mo <2 to 98 Se	Snakepit vent field, MAR	Hannington et al. (1991)
49	100		100	1200-1800	1000			400-3000	Avg 300 Ni	Rainbow vent field, MAR	Marques et al. (2006)
40 38		224 257			 500	 bdl	4.94 bdl	 937.5	Avg 25.2 Se, 0.25 Au, 1.2 Te	Turtle Pits, MAR Turtle Pits, MAR	Wohlgemuth-Ueberwasser et al. (2015)
23 6		326 bdl			 300	 bdl	11.2 bdl	 bdl	Avg 15.5 Se, 4.18 Au, 0.58 Te	Logatchev, MAR Logatchev, MAR	Wohlgemuth-Ueberwasser et al. (2015)
3	18	664.3	26.6	36			10.3		20-200 Se	Southern Explorer Ridge	Hannington et al. (1991)
16	<200	600	<200	200	3600	200	<200	1300	Avg 400 Ni Avg 200 Se	Kairei vent field, Indian Ridge	Wang et al. (2014)
19	143	224	8.71	110	500	444	3.91	300	Avg 538 Mn Avg 36.4 Se	Wocan hydrothermal field, Carlsberg Ridge, Indian Ocean	Wang et al. (2017)
6		800-2600		1000-12100	800-2400					Green Seamount, EPR	Alt et al. (1987)
339	<200	2950	<200		2300	3350	450	550	Max 6900 Hg, Avg <300	Palinuro Volcanic Complex, Aeolian Arc, Italy	Petersen et al. (2014)
3			0-100	400-600	500-11700			0-3500	0 Ni	Alice Spring Field, Mariana Trough	Iwaida and Ueno (2005)

No.	Ag	As	Cd	Co	Cu	Pb	Sb	Zn	Other	Location (setting)	Authors
3		0-500							0-200 Au	North Knoll, Iheya Ridge, Okinawa Trough	Ueno et al. (2003)
58		2635					188		Avg 7.39 Se, 7.71 Au, 1.1 Te	Roman Ruins, Pacmanus Basin, PNG	
44		3636			2200	3236	144	4981		Roman Ruins, Pacmanus Basin, PNG	Wohlgemuth-Ueberwasser et al. (2015)
5		5390					29.4		Avg 5.97 Se, 8.16 Au, bdl Te	Satanic Mills, Pacmanus Basin, PNG	
2		bdl			8200	4100	bdl	2900		Satanic Mills, Pacmanus Basin, PNG	
Sphalerite ((ZnFe)S)											
34	0-1700	0-10100	0-9000		0-7900	0	0-1300		0-900 In, Ni 3600-18000 Fe	Menez Gwen Field, MAR	Lein et al. (2010)
3	49-206	66-93	599-1646	55-101			25-56		<0.1-5.7 Au <1-30 Mo, <2-23 Se	TAG hydrothermal field, MAR	Hannington et al. (1991)
88	<400 – 917		1400-3076		1804-9988	<1000 – 1600	<400 - 900		6094-34006 Fe <300 Mn	TAG hydrothermal field, MAR	Tivey et al. (1995)
2	430-1147	769-881	515-829	7-18			138-163		10.7-18.3 Au 25-29 Mo, <2 Se	Snakepit vent field, MAR	Hannington et al. (1991)
5	1000		600	100	2200				Avg 14000 Fe	Rainbow vent field, MAR	Marques et al. (2006)
20		147					47.9		0.36 Au, 28.2 Se, 0.62 Te	Turtle Pits, MAR	Wohlgemuth-Ueberwasser et al. (2015)
6		100			1450	bdl	bdl		142000 Fe	Turtle Pits, MAR	
10		214					223		3.73 Au, 1.68 Se, 0.73 Te	Logatchev, MAR	Wohlgemuth-Ueberwasser et al. (2015)
8		300			11400	bdl	300		114500 Fe	Logatchev, MAR	
12	<200	400	1000	400	9000	1500	<200		Avg 62900 Fe <200 Ni, Se	Kairei vent field, Indian Ridge	Wang et al. (2014)
17	96.9	726	3085	0.06	12530	1718	86		Avg 16066 Fe Avg 131 Ga, 200 Ge	Wocan hydrothermal field, Carlsberg Ridge, Indian Ocean	Wang et al. (2017)
65	4200	6600	2100		13400	4600	<200		Avg 1200 Fe, 600 Ga Avg 2700 Hg, 300 Tl	Hook Ridge, Antarctica	Petersen et al. (2004)
6			5700-11900		700-5600				2900-77100 Fe	Green Seamount, EPR	Alt et al. (1987)
5	210-400	108-364	1820-3150				355-1580		1.1-3.1 Au	Axial Seamount, JDFR	Hannington et al. (1991)
					0-10000				<10000-80000 Fe		Hannington and Scott (1988)
34	0-2100		0-5600		0-5100				3500-117000 Fe	Southern JDFR	Paradis et al. (1988)
30			300-3500						700-187000 Fe	North Cleft, JDFR	Koski et al. (1994)
3			0-4400		0-8100				9000-150000 Fe, 0-200 Mn	South Cleft, JDFR	Normark et al. (1983)
311	<200	4600	3800		2600	12900	2200		Avg 8000 Fe, 7400 Hg	Palinuro Volcanic Complex, Aeolian Arc, Italy	Petersen et al. (2014)
6		0-1000	5200-6300		800-6500				500-4300 Fe	Hakurei Deposit, Bayonnaise Knoll, Uzu-Bonin Arc	Watanabe and Hayashi (2014)
4			500-5300		1800-12300				189100-236100 Fe 6300-120400 Mn	Escanaba Trough, Gorda Ridge	Zierenberg and Shanks (1983)

No.	Ag	As	Cd	Co	Cu	Pb	Sb	Zn	Other	Location (setting)	Authors
15					3000-7000				<1000-27000 Fe <1000-4000 Mn	Central Okinawa Trough	Halbach et al. (1993)
8			1200-3300	0-300	0-500				10900-26200 Fe 1600-4700 Mn, 0-600 Ni	North Knoll, Iheya Ridge, Okinawa Trough	Ueno et al. (2003)
82			400-900		1100-13700				2100-106800 Fe 2600-15600 Mn	Yonaguni Knoll, Okinawa Trough	Suzuki et al. (2008)
7			200-5000		0-8900				2900-58200 Fe 100-1200 Mn	Alice Spring Field, Mariana Trough	Iwaida and Ueno (2005)
			300-1700						150600-241200 Fe 900-7000 Mn	Guaymas Basin, Gulf of California	Koski et al. (1985)
7	700	11000			38000	15000	<500		20000 Fe	Pacmanus Chimney, PNG	Binns and Scott (1993)
52		1664					1576		43.3 Au, 3.57 Se, 0.02 Te	Roman Ruins, Pacmanus, PNG	Wohlgemuth-Ueberwasser et al. (2015)
24		1216.6			3433.3	1760	1700		35766.6 Fe	Roman Ruins, Pacmanus, PNG	
6		17269					167		2.45 Au, 9.42 Se, bdl Te	Satanic Mills, Pacmanus, PNG	
3		1600			5600	23500	100		7000 Fe	Satanic Mills, Pacmanus, PNG	
Sphalerite – Wurtzite ((ZnFe)S)											
30					bdl-38500				45300-119200 Fe 500-3300 Mn	Mothra hydrothermal field, JDFR	Kristall et al. (2006)
44	<400	<300 – 400	1580	<200	<700-9100	<1000 – 2550	<400		<300 – 6542 Mn <500 – 246793 Fe	Endeavour Segment, JDFR	Tivey et al. (1999)
Wurtzite ((ZnFe)S)											
7	0-900		400-7100		1500-8100				65200-165500 Fe	Southern JDFR	Paradis et al. (1988)
33			1150-7000						32100-175000 Fe	North Cleft, JDFR	Koski et al. (1994)
2			0-2900		0				36000-128000 Fe	South Cleft, JDFR	Normark et al. (1983)
4			1700-4200	0-600	0-2200				21600-60700 Fe 4600-10000 Mn 0-700 Ni	North Knoll, Iheya Ridge, Okinawa Trough	Ueno et al. (2003)
19			1500		1900				28800 Fe 3200 Mn	Yonaguni Knoll, Okinawa Trough	Suzuki et al. (2008)
Chalcopyrite ($CuFeS_2$)											
	58-378		2-258			0-379	0-110.83	180-26100	0-129 Mn 0.32-953 Mo 101-770 Se 0-116.2 V	Menez Gwen Field, MAR	Lein et al. (2010)
	13-48	6-65	<10	113-1053			0.4-5		0.2-0.9 Au 98-498 Co 205-640 Se	TAG hydrothermal field, MAR	Hannington et al. (1991)
90	<400			<400		<1000		1223-9820	<300 – 1060 Se	TAG hydrothermal field, MAR	Tivey et al. (1995)
35	100-700		200-600	200-2000				1300-12100	100-400 Ni	Rainbow vent field, MAR	Marques et al. (2006)

No.	Ag	As	Cd	Co	Cu	Pb	Sb	Zn	Other	Location (setting)	Authors
10	150			3150				416	1150 Au 1400 Ni		Mozgova et al. (2005)
15		37.9					0.46		0.06 Au, 204 Se, 4.73 Te	Turtle Pits, MAR	Wohlgemuth-Ueberwasser et al. (2015)
24		bdl				bdl	bdl	1140		Turtle Pits, MAR	
29		92.4					22		3.12 Au, 119 Se, 39.2 Te	Logatchev, MAR	Wohlgemuth-Ueberwasser et al. (2015)
18		300				bdl	100	1550		Logatchev, MAR	
	<5	49-100	<10	19-383			0.6-0.7		<0.1 Au 77-443 Mo 190-310 Se	Southern Explorer Ridge	Hannington et al. (1991)
33	<200	<200	<200	<200		<200	<200	100	<200 Ni 300 Se	Kairei vent field, Indian Ridge	Wang et al. (2014)
22	65.3	225	46.9	0.1		120	22	1040	Avg 50 Se Avg 80.8 Ge	Wocan hydrothermal field, Carlsberg Ridge, Indian Ocean	Wang et al. (2017)
	100-1500		100-700					1700-10400		Southern Juan de Fuca Ridge	Paradis et al. (1988)
105	<200	<1000	<200			<2000	900	300	100 Hg	Palinuro Volcanic Complex, Aeolian Arc, Italy	Petersen et al. (2014)
4			125					3925	100 Mn	Alice Spring Field, Mariana Trough	Iwaida and Ueno (2005)
4			0					14850	400 Mn	North Knoll, Iheya Ridge, Okinawa Trough	Ueno et al. (2003)
5	<500	800				<1400	<400	<500		Pacmanus Chimney, PNG	Binns and Scott (1993)
75		470					84.5		4.84 Au, 23.5 Se, 0.32 Te	Roman Ruins, Pacmanus, PNG	Wohlgemuth-Ueberwasser et al. (2015)
43		bdl				160	100	2350		Roman Ruins, Pacmanus, PNG	
25		15237					875		4.99 Au, 1.39 Se, 1.66 Te	Satanic Mills, Pacmanus, PNG	
15		bdl				200	300	5850		Satanic Mills, Pacmanus, PNG	
Chalcopyrite ($CuFeS_2$) – Isocubanite ($CuFe_2S_3$)											
64	<400	<400 – 600		<400		<1000	<100	1600 – 12150	<400 Mn	Endeavour Segment, JDFR	Tivey et al. (1999)
Isocubanite ($CuFe_2S_3$)											
10		22.4					7.63		8.15 Au, 40.9 Se, 7.9 Te	Logatchev, MAR	Wohlgemuth-Ueberwasser et al. (2015)
8		bdl				bdl	bdl	5300		Logatchev, MAR	
32	100-300		100-300	700-5200				300-3100	100-700 Ni	Rainbow vent field, MAR	Marques et al. (2006)
2	<200-200	<200-400	<200	1050		<200	<200	1550	<200 Ni 1400-2000 Se	Kairei vent field, Indian Ridge	Wang et al. (2014)
	400-900		100-700					3800-7100		Southern JDFR	Paradis et al. (1988)
Chalcocite (Cu_2S)											
15		43.5					17.8		4.92 Au, 87.9 Se, 4.4 Te	Logatchev, MAR	Wohlgemuth-Ueberwasser et al. (2015)
5		749					304		4.16 Au, bdl Se, 0.69 Te	Satanic Mills, Pacmanus, PNG	Wohlgemuth-Ueberwasser et al. (2015)
Bornite (Cu_5FeS_4)											
3	1700	<400				<1400	<600			Pacmanus Chimney, PNG	Binns and Scott (1993)
11	230	9.97	5.56	0.06		84.4	4.57	200	0.826 Au 9.24 Ge	Wocan hydrothermal field, Carlsberg Ridge, Indian Ocean	Wang et al. (2017)

No.	Ag	As	Cd	Co	Cu	Pb	Sb	Zn	Other	Location (setting)	Authors
Chalcocite-Covellite (Cu_2S-CuS)											
12 14		6.75 100				 bdl	1.38 100	 100	0.55 Au, 7.3 Te	Logatchev, MAR Logatchev, MAR	Wohlgemuth-Ueberwasser et al. (2015)
Covellite (CuS)											
3	0-700	0-3700	0-300	0-500			0-10	0-400	0-1 Au, 100 In, 6-300 Mn 1-300 Mn	Menez Gwen Field, MAR	Lein et al. (2010)
8	<200	<200	<200	<200-200		<200	<200	<200	<200-200 Ni <200-500 Se	Kairei vent field, Indian Ridge	Wang et al. (2014)
2	1050	<200					200	1100	150 Hg, <200 Se	Hook Ridge, Antarctica	Petersen et al. (2004)
Digenite (Cu_9S_5)											
9	<200	<200	<200	<200		<200	<200	<200	<200 Ni, <200 Se	Kairei vent field, Indian Ridge	Wang et al. (2014)
11	350	17.7	5.39	0.08		77.5	3.12	b.d.l.	Avg 41000 Fe 5.45 Ga, 4.78 Ge	Wocan hydrothermal field, Carlsberg Ridge, Indian Ocean	Wang et al. (2017)
Enargite (Cu_3AsS_4)											
10	500						300	9400	5200 Fe, 300 Hg, 1000 Se	Hook Ridge, Antarctica	Petersen et al. (2004)
30	2800		<200			13100	13300	17800	12400 Fe, 5100 Hg	Palinuro Volcanic Complex, Aeolian Arc, Italy	Petersen et al. (2014)
3						700-14600	0-700	3300-15800	2700-8400 Fe	Hakurei Deposit, Bayonnaise Knoll, Uzu-Bonin-Arc	Watanabe and Hayashi (2014)
25	200-7400		0-100				200-2400		100-3500 Fe 100-700 Mn, 200-500 Mo	Yonaguni Knoll, Okinawa Trough	Suzuki et al. (2008)
Tennantite/Tetrahedrite ($Cu_{12}As_4S_{13}$-$Cu_{12}Sb_4S_{13}$)											
38	8000	178500				4500	20900	88500	3800 Fe, 1000 Hg, 900 Se	Hook Ridge, Antarctica	Petersen et al. (2004)
368	2700	40400	<200			<2000	241800	24000	42100 Fe, 4400 Hg	Palinuro Volcanic Complex, Aeolian Arc, Italy	Petersen et al. (2014)
	1600-3600	166300-198400					0-34500	72800-96400	7200-7700 Fe	Hakurei Deposit, Bayonnaise Knoll, Uzu-Bonin-Arc	Watanabe and Hayashi (2014)
8 5 28	10000-73250 74600 1800-33600	56500-124500 71120 99500-133500	 0-200			 	17250-145000 167440 200-33800	55000-67750 61640 51000-59600	2000-6000 Fe 11080 Fe, 1140 Mn 5500-8000 Fe, 400-15300 Mn	Central Okinawa Trough North Knoll, Iheya Ridge, Okinawa Trough Yonaguni Knoll, Okinawa Trough	Halbach et al. (1993) Ueno et al. (2003) Suzuki et al. (2008)
7 7 5	1100-1600 	188000-191000 81298 198500	 			3500-6900 750	900-1200 3609 5650	25000-47000 18550	46000-64000 Fe 15.9 Au, <5 Se, 0.5 Te 61850 Fe	Pacmanus Chimney, PNG Satanic Mills, Pacmanus, PNG Satanic Mills, Pacmanus, PNG	Binns and Scott (1993) Wohlgemuth-Ueberwasser et al. (2015)
Galena (PbS)											
24	100	<200	1100		1800		<200	3400	<200 Fe, <200 Ga, <200 Hg <200 Se	Hook Ridge, Antarctica	Petersen et al. (2004)
36	500	<1000	800		300		9400	2300	300 Fe, 200 Hg	Palinuro Volcanic Complex, Aeolian Arc, Italy	Petersen et al. (2014)
3	1266.6				966.6		1100			Alice Spring Field, Mariana Trough	Iwaida and Ueno (2005)
5 83	2160 200-1800				320 700-		2740			North Knoll, Iheya Ridge, Okinawa Trough Yonaguni Knoll, Okinawa Trough	Ueno et al. (2003) Suzuki et al. (2008)

No.	Ag	As	Cd	Co	Cu	Pb	Sb	Zn	Other	Location (setting)	Authors
					7700						
7	600							2000	4416 Fe, 557 Se	Endeavour Segment, JDFR	Tivey et al. (1999)

8 Acknowledgements

We would like to thank The Engineering and Physical Sciences Research Council (EPSRC) and Ascension Holdings Ltd (AHL) for financially supporting this research.

9 References

Abraitis, P.., Pattrick, R.A.D., Kelsall, G.H., Vaughan, D.J., 2004a. Acid leaching and dissolution of major sulphide ore minerals: processes and galvanic effects in complex systems. Mineral. Mag. 68, 343–351. doi:10.1180/0026461046820191

Abraitis, P.., Pattrick, R.A.D., Vaughan, D.J., 2004b. Variations in the compositional, textural and electrical properties of natural pyrite: a review. Int. J. Miner. Process. 74, 41–59. doi:10.1016/j.minpro.2003.09.002

Acero, P., Cama, J., Ayora, C., 2007. Sphalerite dissolution kinetics in acidic environment. Appl. Geochemistry 22, 1872–1883. doi:10.1016/j.apgeochem.2007.03.051

Acero, P., Cama, J., Ayora, C., Asta, M.P., 2009. Chalcopyrite dissolution rate law from pH 1 to 3. Geol. Acta 7, 389–397. doi:10.1344/105.000001444

Adam, K., Natarajan, K.A., Iwasaki, I., 1984. Grinding media wear and its effect on the flotation of sulfide minerals. Int. J. Miner. Process. 12, 39–54. doi:10.1016/0301-7516(84)90021-8

Ahonen, L., Hiltunen, P., Tuovinen, O., 1985. The role of pyrrhotite and pyrite in the bacterial leaching of chalcopyrite ores, in: Branion, R.M.R., Ebner, H.G. (Eds.), Fundamental and Applied Biohydrometallurgy. Amsterdam, pp. 13–22.

Alt, J.C., Lonsdale, P., Haymon, R., Muehlenbachs, K., 1987. Hydrothermal sulfide and oxide deposits on seamounts near 21°N, East Pacific Rise. Geol. Soc. Am. Bull. 98, 157–168. doi:10.1130/0016-7606(1987)98

Ando, T., Yamamoto, M., Tomiyasu, T., Hashimoto, J., Miura, T., Nakano, A., Akiba, S., 2002. Bioaccumulation of mercury in a vestimentiferan worm living in Kagoshima Bay, Japan. Chemosphere 49, 477–484. doi:10.1016/S0045-6535(02)00291-6

Andrew, R.L., 1984. The geochemistry of selected base-metal gossans, southern Africa. J. Geochemical Explor. 22, 161–192. doi:10.1016/0375-6742(84)90011-6

Antonijević, M.M., Dimitrijević, M., Janković, Z., 1997. Leaching of pyrite with hydrogen peroxide in sulphuric acid. Hydrometallurgy 46, 71–83. doi:10.1016/S0304-386X(96)00096-5

Arnold, R.G., 1967. Range in composition and structure of 82 natural terrestrial pyrrhotites. Can. Mineral. 9, 31–50.

Arora, H.S., Dixon, J.B., Hossner, L.R., 1978. Pyrite morphology in lignitic coal and associated strata of east Texas. Soil Sci. 125, 151–159.

Atapour, H., Aftabi, A., 2007. The geochemistry of gossans associated with Sarcheshmeh porphyry copper deposit, Rafsanjan, Kerman, Iran: Implications for exploration and the environment. J. Geochemical Explor. 93, 47–65. doi:10.1016/j.gexplo.2006.07.007

Attia, Y.A., El-Zeky, M., 1990. Effects of galvanic interactions of sulfides on extraction of precious metals from refractory complex sulfides by bioleaching. Int. J. Miner. Process. 30, 99–111. doi:10.1016/0301-7516(90)90068-A

Avery, E.R., Benning, L.G., 2008. Direct vs. indirect quantification of pyrite oxidation rates. Geochim. Cosmochim. Acta 72, A38.

Avery, E.R., Benning, L.G., 2007. Pyrite oxidation at seafloor conditions: inorganic mechanisms. Geochemica Cosmochim. Acta 71, A46.

Baker, B.J., Banfield, J.F., 2003. Microbial communities in acid mine drainage. FEMS Microbiol. Ecol. 44, 139–52. doi:10.1016/S0168-6496(03)00028-X

Baldo, G., 1992. An examination of marcasite and pyrite oxidative/dissolution rates in seawater. University of South Florida.

Barrett, T.J., Jarvis, I., Jarvis, K.E., 1990. Rare earth element geochemistry of massive sulfides-sulfates and gossans on the Southern Explorer Ridge. Geology 18, 583–586. doi:10.1130/0091-7613(1990)018

Beaudoin, G., 2000. Acicular sphalerite enriched in Ag, Sb and Cu embedded within color-banded sphalerite from the Kokanee Range, British Columbia, Canada. Can. Mineral. 38, 1387–1398. doi:10.2113/gscanmin.38.6.1387

Becker, U., Rosso, K.M., Hochella, M.F., 2001. The proximity effect on semiconducting mineral surfaces: a new aspect of mineral surface reactivity and surface complexation theory? Geochim. Cosmochim. Acta 65, 2641–2649. doi:10.1016/S0016-7037(01)00624-X

Belzile, N., Chen, Y., Cai, M., Li, Y., 2004. A review on pyrrhotite oxidation. J. Geochemical Explor. 84, 65–76. doi:10.1016/j.gexplo.2004.03.003

Benjamin, M.M., Leckie, J.O., 1981. Multiple-site adsorption of Cd, Cu, Zn, and Pb on amorphous iron oxyhydroxide. J. Colloid Interface Sci. 79, 209–221. doi:10.1016/0021-9797(81)90063-1

Berry, V.K., Murr, L.E., Hiskey, J.B., 1978. Galvanic interaction between chalcopyrite and pyrite during bacterial leaching of low-grade waste. Hydrometallurgy 3, 309–326. doi:10.1016/0304-386X(78)90036-1

Biegler, T., 1976. Oxygen reduction on sulphide minerals. J. Electroanal. Chem. Interfacial Electrochem. 70, 265–275. doi:10.1016/S0022-0728(76)80195-7
Biegler, T., Swift, D.A., 1979. Anodic electrochemistry of chalcopyrite. J. Appl. Electrochem. 9, 545–554. doi:10.1007/BF00610940
Bierens de Haan, S., 1991. A review of the rate of pyrite oxidation in aqueous systems at low temperature. Earth-Science Rev. 31, 1–10. doi:10.1016/0012-8252(91)90039-I
Bilenker, L., 2011. Abiotic Oxidation Rate of Chalcopyrite in Seawater: Implications for Seafloor Mining. University of California Riverside.
Bilenker, L., Romano, G.Y., Mckibben, M.A., 2011. Anthropogenic Oxidation of Seafloor Massive Sulfide (SMS) deposits: Implications for Localized Seafloor Acid Generation, in: American Geophysical Union.
Bilenker, L.D., Romano, G.Y., McKibben, M.A., 2016. Kinetics of sulfide mineral oxidation in seawater: Implications for acid generation during in situ mining of seafloor hydrothermal vent deposits. Appl. Geochemistry 75, 20–31. doi:10.1016/j.apgeochem.2016.10.010
Binns, R.A., Scott, S.D., 1993. Actively forming polymetallic sulfide deposits associated with felsic volcanic rocks in the eastern Manus back-arc basin, Papua New Guinea. Econ. Geol. 88, 2226–2236. doi:10.2113/gsecongeo.88.8.2226
Bonnissel-Gissinger, P., Alnot, M., Ehrhardt, J.-J., Behra, P., 1998. Surface Oxidation of Pyrite as a Function of pH. Environ. Sci. Technol. 32, 2839–2845. doi:10.1021/es980213c
Boschen, R.E., Rowden, A.A., Clark, M.R., Gardner, J.P.A., 2013. Mining of deep-sea seafloor massive sulfides: A review of the deposits, their benthic communities, impacts from mining, regulatory frameworks and management strategies. Ocean Coast. Manag. 84, 54–67. doi:10.1016/j.ocecoaman.2013.07.005
Boschen, R.E., Rowden, A.A., Clark, M.R., Pallentin, A., Gardner, J.P.A., 2016. Seafloor massive sulfide deposits support unique megafaunal assemblages: implications for seabed mining and conservation. Mar. Environ. Res. 115, 78–88. doi:10.1016/j.marenvres.2016.02.005
Bouffard, S.C., Rivera-Vasquez, B.F., Dixon, D.G., 2006. Leaching kinetics and stoichiometry of pyrite oxidation from a pyrite–marcasite concentrate in acid ferric sulfate media. Hydrometallurgy 84, 225–238. doi:10.1016/j.hydromet.2006.05.008
Bruemmer, G.W., Gerth, J., Tiller, K.G., 1988. Reaction kinetics of the adsorption and desorption of nickel, zinc and cadmium by goethite. I. Adsorption and diffusion of metals. J. Soil Sci. 39, 37–52. doi:10.1111/j.1365-2389.1988.tb01192.x
Bull, A.J., Mazzucchelli, R.H., 1974. Application of discriminant analysis to the geochemical evaluation of gossans, in: Geochemical Exploration 1974. Elsevier, Amsterdam, pp. 219–316.
Butler, I.B., Nesbitt, R.W., 1999. Trace element distributions in the chalcopyrite wall of a black smoker chimney: insights from laser ablation inductively coupled plasma mass spectrometry (LA–ICP–MS). Earth Planet. Sci. Lett. 167, 335–345. doi:10.1016/S0012-821X(99)00038-2
Cabri, L.J., Campbell, J.L., Laflamme, J.H.G., Leigh, R.G., Maxwell, J.A., Scott, J.D., 1985. Proton-microprobe analysis of trace elements in sulfides from some massive-sulfide deposits. Can. Mineral. 23, 133–148.
Caldeira, K., Wickett, M.E., 2003. Oceanography: Anthropogenic carbon and ocean pH. Nature 425, 365–365. doi:10.1038/425365a
Cao, L., Zhang, H., Zheng, M., Wang, S., 2014. Response of ocean acidification to a gradual increase and decrease of atmospheric CO2. Environ. Res. Lett. 9, 24012. doi:10.1088/1748-9326/9/2/024012
Chandra, A.P., Gerson, A.R., 2010. The mechanisms of pyrite oxidation and leaching: A fundamental perspective. Surf. Sci. Rep. 65, 293–315. doi:10.1016/j.surfrep.2010.08.003
Chandra, A.P., Gerson, A.R., 2009. A review of the fundamental studies of the copper activation mechanisms for selective flotation of the sulfide minerals, sphalerite and pyrite. Adv. Colloid Interface Sci. 145, 97–110. doi:10.1016/j.cis.2008.09.001
Charlou, J.L., Fouquet, Y., Donval, J.P., Auzende, J.M., Jean-Baptiste, P., Stievenard, M., Michel, S., 1996. Mineral and gas chemistry of hydrothermal fluids on an ultrafast spreading ridge: East Pacific Rise, 17° to 19°S (Naudur cruise, 1993) phase separation processes controlled by volcanic and tectonic activity. J. Geophys. Res. 101, 15899. doi:10.1029/96JB00880
Chen, J., Chen, Y., 2010. A first-principle study of the effect of vacancy defects and impurities on the adsorption of O2 on sphalerite surfaces. Colloids Surfaces A Physicochem. Eng. Asp. 363, 56–63. doi:10.1016/j.colsurfa.2010.04.013
Chen, J., Wang, L., Chen, Y., Guo, J., 2011. A DFT study of the effect of natural impurities on the electronic structure of galena. Int. J. Miner. Process. 98, 132–136. doi:10.1016/j.minpro.2010.11.001
Chen, Y., Chen, J., Guo, J., 2010. A DFT study on the effect of lattice impurities on the electronic structures and floatability of sphalerite. Miner. Eng. 23, 1120–1130. doi:10.1016/j.mineng.2010.07.005
Cheng, X., Iwasaki, I., 1992. Pulp Potential and Its Implications to Sulfide Flotation. Miner. Process. Extr. Metall. Rev. 11, 187–210. doi:10.1080/08827509208914206
Cherkashev, G.A., Ivanov, V.N., Bel'tenev, V.I., Lazareva, L.I., Rozhdestvenskaya, I.I., Samovarov, M.L., Poroshina, I.M., Sergeev, M.B., Stepanova, T. V., Dobretsova, I.G., Kuznetsov, V.Y., 2013. Massive sulfide ores of the northern equatorial Mid-Atlantic Ridge. Oceanology 53, 607–619. doi:10.1134/S0001437013050032
Chizhikov, D.M., Kovylina, V.N., 1956. Investigations of potentials and anodic polarization of the sulfides and their alloys, in: Proceedings of the 4th Conference on Electrochemistry. Izdanja Akademii Nauk SSSR, Trudy Chetvertogo Soveshchaniya Po Electrokhimii. pp. 715–719.
Clarke, P., Fornasiero, D., Ralston, J., Smart, R.S.C., 1995. A study of the removal of oxidation products from sulfide mineral surfaces. Miner. Eng. 8, 1347–1357. doi:10.1016/0892-6875(95)00101-U
Constantin, C.A., Chiriţă, P., 2013. Oxidative dissolution of pyrite in acidic media. J. Appl. Electrochem. 43, 659–666. doi:10.1007/s10800-013-0557-y
Corkhill, C.L., 2008. The mineralogical and biogeochemical transformations associated with As-bearing sulphide minerals in acid mine drainage system. The University of Manchester.
Da Silva, G., Lastra, M.R., Budden, J.R., 2003. Electrochemical passivation of sphalerite during bacterial oxidation in the presence of galena. Miner. Eng. 16, 199–203. doi:10.1016/S0892-6875(03)00010-4
Dekov, V., Boycheva, T., Hålenius, U., Petersen, S., Billström, K., Stummeyer, J., Kamenov, G., Shanks, W., 2011. Atacamite and paratacamite from the ultramafic-hosted Logatchev seafloor vent field (14°45′N, Mid-Atlantic

Ridge). Chem. Geol. 286, 169–184. doi:10.1016/j.chemgeo.2011.05.002
Desbruyères, D., Biscoito, M., Caprais, J.-C., Colaço, A., Comtet, T., Crassous, P., Fouquet, Y., Khripounoff, A., Le Bris, N., Olu, K., Riso, R., Sarradin, P.-M., Segonzac, M., Vangriesheim, A., 2001. Variations in deep-sea hydrothermal vent communities on the Mid-Atlantic Ridge near the Azores plateau. Deep Sea Res. Part I Oceanogr. Res. Pap. 48, 1325–1346. doi:10.1016/S0967-0637(00)00083-2
Descostes, M., Vitorge, P., Beaucaire, C., 2004. Pyrite dissolution in acidic media. Geochim. Cosmochim. Acta 68, 4559–4569. doi:10.1016/j.gca.2004.04.012
Dichmann, T.K., Finch, J.A., 2001. The role of copper ions in sphalerite-pyrite flotation selectivity. Miner. Eng. 14, 217–225. doi:10.1016/S0892-6875(00)00177-1
Dimitrijevic, M., Antonijevic, M.M., Jankovic, Z., 1996. Kinetics of pyrite dissolution by hydrogen peroxide in perchloric acid. Hydrometallurgy 42, 377–386. doi:10.1016/0304-386X(95)00094-W
Drew, L.W., 2009. The Promise and Perils of Seafloor Mining. Oceanus 47.
Dutrizac, J., Pratt, A., Chen, T., 2003. The mechanism of sphalerite dissolution in ferric sulphate-sulphuric acid media, in: Yazawa International Symposium, Metallurgical and Materials Processing: Principles and Technologies, Aqueous and Electrochemical Processing, Vol. III. pp. 139–161.
Dutrizac, J.E., 1982. Ferric ion leaching of chalcopyrites from different localities. J. Electron. Mater. 13, 303–309. doi:10.1007/BF02667745
Dutrizac, J.E., MacDonald, R.J.C., 1973. The effect of some impurities on the rate of chalcopyrite dissolution. Can. Metall. Q. 12, 409–420.
Dyment, J., Szitkar, F., Fouquet, Y., Choi, Y., 2011. Deep-Sea Magnetics on Active and Fossil Hydrothermal Sites: a Tool to Detect and Characterize Submarine Ore Deposits, in: American Geophysical Union.
Dymond, J., Roth, S., 1988. Plume dispersed hydrothermal particles: A time-series record of settling flux from the Endeavour Ridge using moored sensors. Geochim. Cosmochim. Acta 52, 2525–2536. doi:10.1016/0016-7037(88)90310-9
Edgcomb, V.P., Molyneaux, S.J., Saito, M.A., Lloyd, K., Boer, S., Wirsen, C.O., Atkins, M.S., Teske, A., 2004. Sulfide Ameliorates Metal Toxicity for Deep-Sea Hydrothermal Vent Archaea. Appl. Environ. Microbiol. 70, 2551–2555. doi:10.1128/AEM.70.4.2551-2555.2004
Edwards, K.J., 2004. Formation and degradation of seafloor hydrothermal sulphide deposits. Geol. Soc. Am. Spec. Pap. 379, 83–96. doi:10.1130/0-8137-2379-5.83
Edwards, K.J., McCollom, T.M., Konishi, H., Buseck, P.R., 2003. Seafloor bioalteration of sulfide minerals: results from in situ incubation studies. Geochim. Cosmochim. Acta 67, 2843–2856. doi:10.1016/S0016-7037(03)00089-9
Ekmekçi, Z., Demirel, H., 1997. Effects of galvanic interaction on collectorless flotation behaviour of chalcopyrite and pyrite. Int. J. Miner. Process. 52, 31–48. doi:10.1016/S0301-7516(97)00050-1
Ellmer, K., Höpfner, C., 2006. On the stoichiometry of the semiconductor pyrite (FeS2). Philos. Mag. A 75, 1129–1151. doi:10.1080/01418619708214015
Erickson, K.L., Macko, S.A., Van Dover, C.L., 2009. Evidence for a chemoautotrophically based food web at inactive hydrothermal vents (Manus Basin). Deep Sea Res. Part II Top. Stud. Oceanogr. 56, 1577–1585. doi:10.1016/j.dsr2.2009.05.002
Evangelou, V.P. (Bill), Zhang, Y.L., 1995. A review: Pyrite oxidation mechanisms and acid mine drainage prevention. Crit. Rev. Environ. Sci. Technol. 25, 141–199. doi:10.1080/10643389509388477
Feely, R.A., Geiselman, T.L., Baker, E.T., Massoth, G.J., Hammond, S.R., 1990. Distribution and Composition of Hydrothermal Plume Particles From the ASHES Vent Field at Axial Volcano, Juan de Fuca Ridge. J. Geophys. Res. 95873, 855–12. doi:10.1029/JB095iB08p12855
Feely, R.A., Lewison, M., Massoth, G.J., Robert-Baldo, G., Lavelle, J.W., Byrne, R.H., Von Damm, K.L., Curl, H.C., 1987. Composition and dissolution of black smoker particulates from active vents on the Juan de Fuca Ridge. J. Geophys. Res. 92, 11347. doi:10.1029/JB092iB11p11347
Feely, R.A., Orr, J., Fabry, V.J., Kleypas, J.A., Sabine, C.L., Langdon, C., 2009. Present and future changes in seawater chemistry due to ocean acidification, in: Mcpherson, B.J., Sundquist, E.T. (Eds.), AGU Monograph on "The Science and Technology of Carbon Sequestration'. American Geophysical Union, pp. 175–188. doi:10.1029/2005GM000337
Fowler, T.A., Holmes, P.R., Crundwell, F.K., 1999. Mechanism of pyrite dissolution in the presence of Thiobacillus ferrooxidans. Appl. Environ. Microbiol. 65, 2987–93.
Fullston, D., Fornasiero, D., Ralston, J., 1999. Zeta potential study of the oxidation of copper sulfide minerals. Colloids Surfaces A Physicochem. Eng. Asp. 146, 113–121. doi:10.1016/S0927-7757(98)00725-0
Garrels, R.M., Thompson, M.E., 1960. Oxidation of pyrite by iron sulfate solutions. Am. J. Sci. 258, 57–67.
Gartman, A., Luther, G.W., 2014. Oxidation of synthesized sub-micron pyrite (FeS2) in seawater. Geochim. Cosmochim. Acta 144, 96–108. doi:10.1016/j.gca.2014.08.022
Gena, K., 2013. Deep Sea Mining of Submarine Hydrothermal Deposits and its Possible Environmental Impact in Manus Basin, Papua New Guinea. Procedia Earth Planet. Sci. 6, 226–233. doi:10.1016/j.proeps.2013.01.031
German, C.R., Petersen, S., Hannington, M.D., 2016. Hydrothermal exploration of mid-ocean ridges: Where might the largest sulfide deposits be forming? Chem. Geol. 420, 114–126. doi:10.1016/j.chemgeo.2015.11.006
German, C.R., Sparks, R.S.J., 1993. Particle recycling in the TAG hydrothermal plume. Earth Planet. Sci. Lett. 116, 129–134. doi:10.1016/0012-821X(93)90049-F
Gigowski, B., Vogg, A., Wierer, K., Dobias, B., 1991. Effect of Fe-lattice ions on adsorption, electrokinetic, calorimetric and flotation properties of sphalerite. Int. J. Miner. Process. 33, 103–120. doi:10.1016/0301-7516(91)90046-L
Goulding, H.C., Mills, R.A., Nesbitt, R.W., 1998. Precipitation of hydrothermal sediments on the active TAG mound: implications for ochre formation, in: Modern Ocean Floor Processes and the Geological Record. Geological Society, London, Special Publications, pp. 201–216.
Guinotte, J.M., Fabry, V.J., 2008. Ocean Acidification and Its Potential Effects on Marine Ecosystems. Ann. N. Y. Acad. Sci. 1134, 320–342. doi:10.1196/annals.1439.013
Gupta, V.P., Ravindra, N.M., Srivastava, V.K., 1980. Semiconducting properties of pyrite. J. Phys. Chem. Solids 41, 145–148. doi:10.1016/0022-3697(80)90046-3
Gwyther, D., 2008a. Environmental Impact Statement, Solwara 1 Project, in: Executive Summary Coffey Natural

Systems. Brisbane.
Gwyther, D., 2008b. Environmental Impact Statement, Solwara 1 Project, in: Main Report Coffey Natural Systems. Brisbane.
Haase, K.M., Petersen, S., Koschinsky, A., Seifert, R., Devey, C.W., Keir, R., Lackschewitz, K.S., Melchert, B., Perner, M., Schmale, O., Süling, J., Dubilier, N., Zielinski, F., Fretzdorff, S., Garbe-Schönberg, D., Westernströer, U., German, C.R., Shank, T.M., Yoerger, D., Giere, O., Kuever, J., Marbler, H., Mawick, J., Mertens, C., Stöber, U., Walter, M., Ostertag-Henning, C., Paulick, H., Peters, M., Strauss, H., Sander, S., Stecher, J., Warmuth, M., Weber, S., 2007. Young volcanism and related hydrothermal activity at 5°S on the slow-spreading southern Mid-Atlantic Ridge. Geochemistry, Geophys. Geosystems 8. doi:10.1029/2006GC001509
Halbach, P., Pracejus, B., Maerten, A., 1993. Geology and mineralogy of massive sulfide ores from the central Okinawa Trough, Japan. Econ. Geol. 88, 2210–2225. doi:10.2113/gsecongeo.88.8.2210
Hannington, M., Galley, A., 1998. Comparison of the TAG Mound and Stockwork Complex with Cyprus-Type Massive Sulfide Deposits. Proc. Ocean Drill. Program, Sci. Results 158.
Hannington, M., Hall, G., Vaive, J., 1990. Acid pore fluids from an oxidizing sulfide deposit on the Mid-Atlantic Ridge: implications for supergene enrichment of gold on the seafloor. Geol. Soc. Am. Abstr. with Progr. 22, A42.
Hannington, M., Herzig, P., Scott, S., Thompson, G., Rona, P., 1991. Comparative mineralogy and geochemistry of gold-bearing sulfide deposits on the mid-ocean ridges. Mar. Geol. 101, 217–248. doi:10.1016/0025-3227(91)90073-D
Hannington, M., Jamieson, J., 2011. Estimating the metal content of SMS deposits, in: Oceans. IEEE.
Hannington, M., Jamieson, J., Monecke, T., Petersen, S., Beaulieu, S., 2011. The abundance of seafloor massive sulfide deposits. Geology 39, 1155–1158. doi:10.1130/G32468.1
Hannington, M.D., 1993. The formation of atacamite during weathering of sulfides on the modern seafloor. Can. Mineral. 31, 945–956.
Hannington, M.D., de Ronde, C.E.J., Petersen, S., 2005. Modern seafloor tectonics and submarine hydrothermal systems, Economic Geology: One Hundredth Anniversary Volume: 1905-2005. Society of Economic Geologists. doi:10.1029/GM091p0115
Hannington, M.D., Jamieson, J., Monecke, T., Petersen, S., 2010. Modern Sea-Floor Massive Sulfides and Base Metal Resources: Toward an Estimate of Global Sea-Floor Massive Sulfide Potential. Soc. Econ. Geol. Spec. Publ. 15 15, 317–338.
Hannington, M.D., Jonasson, I.R., 1992. Fe and Mn oxides at seafloor hydrothermal vents, in: Skinner, H.C. (Ed.), Biomineralization Processes of Iron and Manganese; Modern and Ancient Environments. pp. 351–370.
Hannington, M.D., Scott, S.D., 1988. Mineralogy and geochemistry of a hydrothermal silica-sulfide-sulfate spire in the caldera of Axial Seamount, Juan De Fuca Ridge. Can. Mineral. 26, 603–625.
Hannington, M.D., Thompson, G., Rona, P.A., Scott, S.D., 1988. Gold and native copper in supergene sulphides from the Mid-Atlantic Ridge. Nature 333, 64–66.
Harmer, S.L., Mierczynska-Vasilev, A., Beattie, D.A., Shapter, J.G., 2008. The effect of bulk iron concentration and heterogeneities on the copper activation of sphalerite. Miner. Eng. 21, 1005–1012. doi:10.1016/j.mineng.2008.02.014
Hawley, J.E., Nichol, I., 1961. Trace elements in pyrite, pyrrhotite and chalcopyrite of different ores. Econ. Geol. 56, 467–487. doi:10.2113/gsecongeo.56.3.467
Haymon, R.M., Kastner, M., 1981. Hot spring deposits on the East Pacific Rise at 21°N: preliminary description of mineralogy and genesis. Earth Planet. Sci. Lett. 53, 363–381. doi:10.1016/0012-821X(81)90041-8
Heidel, C., Tichomirowa, M., Junghans, M., 2013. Oxygen and sulfur isotope investigations of the oxidation of sulfide mixtures containing pyrite, galena, and sphalerite. Chem. Geol. 342, 29–43. doi:10.1016/j.chemgeo.2013.01.016
Hein, J.R., Mizell, K., Koschinsky, A., Conrad, T.A., 2013. Deep-ocean mineral deposits as a source of critical metals for high- and green-technology applications: Comparison with land-based resources. Ore Geol. Rev. 51, 1–14. doi:10.1016/j.oregeorev.2012.12.001
Hekinian, R., 2014. Sea Floor Exploration: Scientific Adventures Diving into the Abyss. Springer International Publishing.
Herzig, P.M., 1999. Economic potential of sea-floor massive sulphide deposits: ancient and modern. Philos. Trans. R. Soc. A Math. Phys. Eng. Sci. 357, 861–875. doi:10.1098/rsta.1999.0355
Herzig, P.M., Hannington, M.D., 1995. Polymetallic massive sulfides at the modern seafloor a review. Ore Geol. Rev. 10, 95–115. doi:10.1016/0169-1368(95)00009-7
Herzig, P.M., Hannington, M.D., Scott, S.D., Maliotis, G., Rona, P.A., Thompson, G., 1991. Gold-rich sea-floor gossans in the Troodos Ophiolite and on the Mid-Atlantic Ridge. Econ. Geol. 86, 1747–1755. doi:10.2113/gsecongeo.86.8.1747
Ho, K.T., Kuhn, A., Pelletier, M.C., Hendricks, T.L., Helmstetter, A., 1999. pH dependent toxicity of five metals to three marine organisms. Environ. Toxicol. 14, 235–240. doi:10.1002/(SICI)1522-7278(199905)14:2<235::AID-TOX4>3.0.CO;2-J
Holmes, P.R., Crundwell, F.K., 2000. The kinetics of the oxidation of pyrite by ferric ions and dissolved oxygen: an electrochemical study. Geochim. Cosmochim. Acta 64, 263–274. doi:10.1016/S0016-7037(99)00296-3
Hönisch, B., Ridgwell, A., Schmidt, D.N., Thomas, E., Gibbs, S.J., Sluijs, A., Zeebe, R., Kump, L., Martindale, R.C., Greene, S.E., Kiessling, W., Ries, J., Zachos, J.C., Royer, D.L., Barker, S., Marchitto, T.M., Moyer, R., Pelejero, C., Ziveri, P., Foster, G.L., Williams, B., 2012. The geological record of ocean acidification. Science. 335, 1058–1063. doi:10.1126/science.1208277
Hu, Y., Sun, W., Wang, D., 2010. Electrochemistry of Flotation of Sulphide Minerals. Springer Science & Business Media.
Huminicki, D.M.C., Rimstidt, J.D., 2009. Iron oxyhydroxide coating of pyrite for acid mine drainage control. Appl. Geochemistry 24, 1626–1634. doi:10.1016/j.apgeochem.2009.04.032
Iwaida, C., Ueno, H., 2005. Ore and gangue minerals of seafloor hydrothermal deposits in the Mariana trough. JAMSTEC Rep. Res. Dev. 1, 1–12.
Iwasaki, I., 1989. Bridging theory and practice in iron ore flotation, in: Advances in Coal and Mineral Processing Using Floatation. pp. 177–190.

Jamieson, H.E., Walker, S.R., Parsons, M.B., 2015. Mineralogical characterization of mine waste. Appl. Geochemistry 57, 85–105. doi:10.1016/j.apgeochem.2014.12.014
Janzen, M.P., Nicholson, R. V, Scharer, J.M., 2000. Pyrrhotite reaction kinetics: reaction rates for oxidation by oxygen, ferric iron, and for nonoxidative dissolution. Geochim. Cosmochim. Acta 64, 1511–1522. doi:10.1016/S0016-7037(99)00421-4
Jeanthon, C., Prieur, D., 1990. Susceptibility to Heavy Metals and Characterization of Heterotrophic Bacteria Isolated from Two Hydrothermal Vent Polychaete Annelids, Alvinella pompejana and Alvinella caudata. Appl. Environ. Microbiol. 56, 3308–14.
Johan, Z., 1988. Indium and germanium in the structure of sphalerite: an example of coupled substitution with Copper. Mineral. Petrol. 39, 211–229. doi:10.1007/BF01163036
Johnson, K.S., Childress, J.J., Beehler, C.L., 1988. Short-term temperature variability in the Rose Garden hydrothermal vent field: an unstable deep-sea environment. Deep Sea Res. Part A. Oceanogr. Res. Pap. 35, 1711–1721. doi:10.1016/0198-0149(88)90045-3
Jyothi, N., Sudha, K.N., Natarajan, K.A., 1989. Electrochemical aspects of selective bioleaching of sphalerite and chalcopyrite from mixed sulphides. Int. J. Miner. Process. 27, 189–203. doi:10.1016/0301-7516(89)90064-1
Karastelev, N., 2013. Modeling of high pressure pretreatment process for gold leaching. Lappeenranta University of Technology.
Kato, S., Takano, Y., Kakegawa, T., Oba, H., Inoue, K., Kobayashi, C., Utsumi, M., Marumo, K., Kobayashi, K., Ito, Y., Ishibashi, J., Yamagishi, A., 2010. Biogeography and biodiversity in sulfide structures of active and inactive vents at deep-sea hydrothermal fields of the Southern Mariana Trough. Appl. Environ. Microbiol. 76, 2968–79. doi:10.1128/AEM.00478-10
Kinsey, J.C., Tivey, M.A., Yoerger, D.R., 2008. Toward high-spatial resolution gravity surveying of the mid-ocean ridges with autonomous underwater vehicles, in: Oceans. IEEE, pp. 1–10. doi:10.1109/OCEANS.2008.5152005
Koleini, S.M.J., Jafarian, M., Abdollahy, M., Aghazadeh, V., 2010. Galvanic Leaching of Chalcopyrite in Atmospheric Pressure and Sulfate Media: Kinetic and Surface Studies. Ind. Eng. Chem. Res. 49, 5997–6002. doi:10.1021/ie100017u
Koski, R.A., Jonasson, I.R., Kadko, D.C., Smith, V.K., Wong, F.L., 1994. Compositions, growth mechanisms, and temporal relations of hydrothermal sulfide-sulfate-silica chimneys at the northern Cleft segment, Juan de Fuca Ridge. J. Geophys. Res. Solid Earth 99, 4813–4832. doi:10.1029/93JB02871
Koski, R.A., Lonsdale, P.F., Shanks, W.C., Berndt, M.E., Howe, S.S., 1985. Mineralogy and geochemistry of a sediment-hosted hydrothermal sulfide deposit from the Southern Trough of Guaymas Basin, Gulf of California. J. Geophys. Res. 90, 6695. doi:10.1029/JB090iB08p06695
Koski, R.A., Munk, L., Foster, A.L., Shanks, W.C., Stillings, L.L., 2008. Sulfide oxidation and distribution of metals near abandoned copper mines in coastal environments, Prince William Sound, Alaska, USA. Appl. Geochemistry 23, 227–254. doi:10.1016/j.apgeochem.2007.10.007
Koslides, T., Ciminelli, V.S.T., 1992. Pressure oxidation of arsenopyrite and pyrite in alkaline solutions. Hydrometallurgy 30, 87–106. doi:10.1016/0304-386X(92)90079-F
Kowalczyk, P., 2011. Geophysical exploration for Submarine Massive Sulfide deposits, in: Oceans. IEEE, pp. 1–5.
Kristall, B., Kelley, D.S., Hannington, M.D., Delaney, J.R., 2006. Growth history of a diffusely venting sulfide structure from the Juan de Fuca Ridge: A petrological and geochemical study. Geochemistry, Geophys. Geosystems 7, 1–30. doi:10.1029/2005GC001166
Kwong, Y.T.J., 1993. Prediction and prevention of acid rock drainage from a geological and mineralogical perspective MEND Project 1.32.1. Ottawa, Canada.
Kwong, Y.T.J., Swerhone, G.W., Lawrence, J.R., 2003. Galvanic sulphide oxidation as a metal-leaching mechanism and its environmental implications. Geochemistry Explor. Environ. Anal. 3, 337–343. doi:10.1144/1467-7873/03/013
Lalou, C., Thompson, G., Arnold, M., Brichet, E., Druffel, E., Rona, P.A., 1990. Geochronology of TAG and Snakepit hydrothermal fields, Mid-Atlantic Ridge: Witness to a long and complex hydrothermal history. Earth Planet. Sci. Lett. 97, 113–128. doi:10.1016/0012-821X(90)90103-5
Lasaga, A.C., 1981. Rate laws of chemical reactions. Rev. Mineral. Geochemistry 8, 1–66.
Le Bris, N., Govenar, B., Le Gall, C., Fisher, C.R., 2006. Variability of physico-chemical conditions in 9°50′N EPR diffuse flow vent habitats. Mar. Chem. 98, 167–182. doi:10.1016/j.marchem.2005.08.008
Le Bris, N., Sarradin, P.-M., Pennec, S., 2001. A new deep-sea probe for in situ pH measurement in the environment of hydrothermal vent biological communities. Deep Sea Res. Part I Oceanogr. Res. Pap. 48, 1941–1951. doi:10.1016/S0967-0637(00)00112-6
Learmont, M.E., Iwasaki, I., 1984. Effect of grinding media on galena flotation. Miner. Metall. Process. 1, 136–143.
Le Roux, S.G., Miller, J.A., Dunford, A.J., Clarke, C.E., 2016. The dissolution kinetics of atacamite in the acid range and the stability of atacamite containing soils from Namaqualand, South Africa. Appl. Geochemistry 64, 22–29. doi:10.1016/j.apgeochem.2015.09.003
Lehner, S., Savage, K., Ciobanu, M., Cliffel, D.E., 2007. The effect of As, Co, and Ni impurities on pyrite oxidation kinetics: An electrochemical study of synthetic pyrite. Geochim. Cosmochim. Acta 71, 2491–2509. doi:10.1016/j.gca.2007.03.005
Lein, A.Y., Bogdanov, Y.A., Maslennikov, V. V., Li, S., Ulyanova, N. V., Maslennikova, S.P., Ulyanov, A.A., 2010. Sulfide minerals in the Menez Gwen nonmetallic hydrothermal field (Mid-Atlantic Ridge). Lithol. Miner. Resour. 45, 305–323. doi:10.1134/S0024490210040012
Lepetit, P., Bente, K., Doering, T., Luckhaus, S., 2003. Crystal chemistry of Fe-containing sphalerites. Phys. Chem. Miner. 30, 185–191. doi:10.1007/s00269-003-0306-6
Levin, L.A., Le Bris, N., 2015. The deep ocean under climate change. Science (80-.). 350, 766–768. doi:10.1126/science.aad0126
Li, Z., Heping, L., Liping, X., 2006. Galvanic interaction between galena and pyrite in an open system. Chinese J. Geochemistry 25, 230–237. doi:10.1007/BF02840416
Linge, H.G., 1977. Reactivity comparison of Australian chalcopyrite concentrates in acidified ferric solution. Hydrometallurgy 2, 219–233. doi:10.1016/0304-386X(77)90003-2
Liu, Q., Li, H., Zhou, L., 2008. Galvanic interactions between metal sulfide minerals in a flowing system: Implications

for mines environmental restoration. Appl. Geochemistry 23, 2316–2323. doi:10.1016/j.apgeochem.2008.02.024
Liu, R., Wolfe, A.L., Dzombak, D.A., Stewart, B.W., Capo, R.C., 2007. Comparison of dissolution under oxic acid drainage conditions for eight sedimentary and hydrothermal pyrite samples. Environ. Geol. 56, 171–182. doi:10.1007/s00254-007-1149-0
Lizama, H.M., Suzuki, I., 1991. Interaction of chalcopyrite and sphalerite with pyrite during leaching by Thiobacillus ferrooxidans and Thiobacillus thiooxidans. Can. J. Microbiol. 37, 304–311. doi:10.1139/m91-047
Lizama, H.M., Suzuki, I., 1989. Rate Equations and Kinetic Parameters of the Reactions Involved in Pyrite Oxidation by Thiobacillus ferrooxidans. Appl. Environ. Microbiol. 55, 2918–23.
Llanos, J., Capasso, C., Parisi, E., Prieur, D., Jeanthon, C., 2000. Susceptibility to Heavy Metals and Cadmium Accumulation in Aerobic and Anaerobic Thermophilic Microorganisms Isolated from Deep-Sea Hydrothermal Vents. Curr. Microbiol. 41, 201–205. doi:10.1007/s002840010119
Long, H., Dixon, D.G., 2004. Pressure oxidation of pyrite in sulfuric acid media: a kinetic study. Hydrometallurgy 73, 335–349. doi:10.1016/j.hydromet.2003.07.010
Lowson, R.T., 1982. Aqueous oxidation of pyrite by molecular oxygen. Chem. Rev. 82, 461–497. doi:10.1021/cr00051a001
Majima, H., 1969. How oxidation affects selective flotation of complex sulphide ores. Can. Metall. Q. 8, 269–273.
Majuste, D., Ciminelli, V.S.T., Osseo-Asare, K., Dantas, M.S.S., 2012. Quantitative assessment of the effect of pyrite inclusions on chalcopyrite electrochemistry under oxidizing conditions. Hydrometallurgy 113–114, 167–176. doi:10.1016/j.hydromet.2011.12.020
Malouf, E.E., Prater, J.D., 1961. Role of bacteria in the alteration of sulfide minerals. J. Met. 13, 353–356.
Marques, A.F.A., Barriga, F., Chavagnac, V., Fouquet, Y., 2006. Mineralogy, geochemistry, and Nd isotope composition of the Rainbow hydrothermal field, Mid-Atlantic Ridge. Miner. Depos. 41, 52–67. doi:10.1007/s00126-005-0040-8
McBeth, J.M., Little, B.J., Ray, R.I., Farrar, K.M., Emerson, D., 2011. Neutrophilic iron-oxidizing “Zetaproteobacteria” and mild steel corrosion in nearshore marine environments. Appl. Environ. Microbiol. 77, 1405–1412. doi:10.1128/AEM.02095-10
McDonald, R.G., Muir, D.M., 2007. Pressure oxidation leaching of chalcopyrite. Part I. Comparison of high and low temperature reaction kinetics and products. Hydrometallurgy 86, 191–205. doi:10.1016/j.hydromet.2006.11.015
McGoldrick, P.J., Keays, R.R., 1981. Precious and volatile metals in the Perseverance nickel deposit gossan; implications for exploration in weathered terrains. Econ. Geol. 76, 1752–1763. doi:10.2113/gsecongeo.76.6.1752
McGuire, M.M., Edwards, K.J., Banfield, J.F., Hamers, R.J., 2001. Kinetics, surface chemistry, and structural evolution of microbially mediated sulfide mineral dissolution. Geochim. Cosmochim. Acta 65, 1243–1258. doi:10.1016/S0016-7037(00)00601-3
McKibben, M.A., Barnes, H.L., 1986. Oxidation of pyrite in low temperature acidic solutions: Rate laws and surface textures. Geochim. Cosmochim. Acta 50, 1509–1520. doi:10.1016/0016-7037(86)90325-X
Mehta, A.P., Murr, L.E., 1983. Fundamental studies of the contribution of galvanic interaction to acid-bacterial leaching of mixed metal sulfides. Hydrometallurgy 9, 235–256. doi:10.1016/0304-386X(83)90025-7
Mehta, A.P., Murr, L.E., 1982. Kinetic study of sulfide leaching by galvanic interaction between chalcopyrite, pyrite, and sphalerite in the presence of T. ferrooxidans (30°C) and a thermophilic microorganism (55°C). Biotechnol. Bioeng. 24, 919–40. doi:10.1002/bit.260240413
Millero, F.J., Hubinger, S., Fernandez, M., Garnett, S., 1987. Oxidation of H2S in seawater as a function of temperature, pH, and ionic strength. Environ. Sci. Technol. 21, 439–43. doi:10.1021/es00159a003
Mills, R., Elderfield, H., Thomson, J., 1993. A dual origin for the hydrothermal component in a metalliferous sediment core from the Mid-Atlantic Ridge. J. Geophys. Res. 98, 9671. doi:10.1029/92JB01414
Monecke, T., Petersen, S., Hannington, M.D., Grant, H., Samson, I., 2016. The minor element endowment of modern sea-floor massive sulfide deposits and comparison with deposits hosted in ancient volcanic successions. Rev. Econ. Geol. 18, 245–306.
Morse, J.W., 1991. Oxidation kinetics of sedimentary pyrite in seawater. Geochim. Cosmochim. Acta 55, 3665–3667. doi:10.1016/0016-7037(91)90064-C
Moses, C.O., Herman, J.S., 1991. Pyrite oxidation at circumneutral pH. Geochim. Cosmochim. Acta 55, 471–482. doi:10.1016/0016-7037(91)90005-P
Moses, C.O., Kirk Nordstrom, D., Herman, J.S., Mills, A.L., 1987. Aqueous pyrite oxidation by dissolved oxygen and by ferric iron. Geochim. Cosmochim. Acta 51, 1561–1571. doi:10.1016/0016-7037(87)90337-1
Mozgova, N.N., Borodaev, Y.S., Gablina, I.F., Cherkashev, G.A., Stepanova, T. V., 2005. Mineral Assemblages as Indicators of the Maturity of Oceanic Hydrothermal Sulfide Mounds. Lithol. Miner. Resour. 40, 293–319. doi:10.1007/s10987-005-0030-z
Murr, L.E., 2006. Biological issues in materials science and engineering: Interdisciplinarity and the bio-materials paradigm. JOM 58, 23–33. doi:10.1007/s11837-006-0136-3
Murton, B., 2013. Seafloor mining: the future or just another pipe dream? Int. J. Soc. Underw. Technol. 31, 53–54. doi:10.3723/ut.31.053
Nakazawa, H., Iwasaki, I., 1986. Galvanic contact between nickel arsenide and pyrrhotite and its effect on flotation. Int. J. Miner. Process. 18, 203–215. doi:10.1016/0301-7516(86)90018-9
Natarajan, K., 1988. Electrochemical aspects of bioleaching multisulfide minerals. Miner. Metall. Process. 5, 61–65.
Natarajan, K.A., 1985. Microbe-mineral interactions of relevance in the hydrometallurgy of complex sulphides, in: Mehrotra, S.P., Ramachandran, T.R. (Eds.), Progress in Metallurgical Research-Fundamental and Applied Aspects. Tata McGraw Hill, New Delhi, New Delhi, pp. 105–112.
Natarajan, K.A., Iwasaki, I., 1983. Role of Galvanic Interactions in the Bioleaching of Duluth Gabbro Copper-Nickel Sulfides. Sep. Sci. Technol. 18, 1095–1111. doi:10.1080/01496398308059919
Natarajan, K., Iwasaki, I., 1986. Microbe-mineral interactions in the leaching of complex Sulfides, in: Clum, J.A., Haas, L.A. (Eds.), Microbiological Effects on Metallurgical Processes. TMS AIME, New York, New York.
Nicholson, R. V., Gillham, R.W., Reardon, E.J., 1988. Pyrite oxidation in carbonate-buffered solution: 1. Experimental kinetics. Geochim. Cosmochim. Acta 52, 1077–1085. doi:10.1016/0016-7037(88)90262-1

Nickel, E.H., 1984. The mineralogy and geochemistry of the weathering profile of the Teutonic Bore Cu-Pb-Zn-Ag sulphide deposit. J. Geochemical Explor. 22, 239–263. doi:10.1016/0375-6742(84)90014-1
Nies, D.H., 1999. Microbial heavy-metal resistance. Appl. Microbiol. Biotechnol. 51, 730–750. doi:10.1007/s002530051457
Nordstrom, D., Alpers, C., 1999. Geochemistry of acid mine waters, in: The Environmental Geochemistry of Mineral Deposits. pp. 133–160.
Normark, W.R., Morton, J.L., Koski, R.A., Clague, D.A., Delaney, J.R., 1983. Active hydrothermal vents and sulfide deposits on the southern Juan de Fuca Ridge. Geology 11, 158. doi:10.1130/0091-7613(1983)11<158:AHVASD>2.0.CO;2
Oertel, J., Ellmer, K., Bohne, W., Röhrich, J., Tributsch, H., 1999. Growth of n-type polycrystalline pyrite (FeS2) films by metalorganic chemical vapour deposition and their electrical characterization. J. Cryst. Growth 198–199, 1205–1210. doi:10.1016/S0022-0248(98)01074-4
Orlova, T.A., Stupnikov, V.M., Krestan, A.L., 1988. Mechanism of oxidative dissolution of sulphides. Zhurnal Prikl. Khimii 61, 2172–2177.
Paradis, S., Jonasson, I.R., Le Cheminant, G.M., Watkinson, D.H., 1988. Two zinc-rich chimneys from the plume site, Southern Juan de Fuca Ridge. Can. Mineral. 26, 637–654.
Parry, D.L., 2008. Solwara 1 Project Elutriate Report Phase 1 and 2.
Parthasarathy, H., Baltrus, J.P., Dzombak, D.A., Karamalidis, A.K., 2014. A method for preparation and cleaning of uniformly sized arsenopyrite particles. Geochem. Trans. 15, 14. doi:10.1186/s12932-014-0014-9
Perez, I.P., Dutrizac, J.., 1991. The effect of the iron content of sphalerite on its rate of dissolution in ferric sulphate and ferric chloride media. Hydrometallurgy 26, 211–232. doi:10.1016/0304-386X(91)90032-H
Peters, E., Majima, H., 1968. The physical chemistry of leaching of sulphide minerals, in: Paper Presented at 97th Annual Meeting AIME, New York.
Peters, S., 2010. An Investigation of the Role of Sodium Carbonate and Silica in the Neutral/Alkaline Pressure Oxidation of Pyrite. University of Toronto.
Petersen, S., Herzig, P.M., Schwarz-Schampera, U., Hannington, M.D., Jonasson, I.R., 2004. Hydrothermal precipitates associated with bimodal volcanism in the Central Bransfield Strait, Antarctica. Miner. Depos. 39, 358–379. doi:10.1007/s00126-004-0414-3
Petersen, S., Monecke, T., Westhues, A., Hannington, M.D., Gemmell, J.B., Sharpe, R., Peters, M., Strauss, H., Lackschewitz, K., Augustin, N., Gibson, H., Kleeberg, R., 2014. Drilling Shallow-Water Massive Sulfides at the Palinuro Volcanic Complex, Aeolian Island Arc, Italy. Econ. Geol. 109, 2129–2158. doi:10.2113/econgeo.109.8.2129
Plumlee, G., Logsdon, M., Filipek, L., 1999. The environmental geology of mineral deposits, in: The Environmental Geochemistry of Mineral Deposits. Society of Economic Geologists, pp. 71–116.
Pollard, A.M., Thomas, R.G., Williams, P.A., 1989. Synthesis and stabilities of the basic copper(II) chlorides atacamite, paratacamite and botallackite 53, 557–563.
Pozzo, R.L., Iwasaki, I., 1989. Pyrite-Pyrrhotite Grinding Media Interactions and Their Effects on Media Wear and Flotation. J. Electrochem. Soc. 136, 1734. doi:10.1149/1.2097001
Pridmore, D., Shuey, R., 1976. The electrical resistivity of galena, pyrite, and chalcopyrite. Am. Mineral. 61, 248–259.
Pugh, C., Hossner, L.R., Dixon, J.B., 1984. Oxidation rate of iron sulfides as affected by surface area, morphology, oxygen concentration, and autotrophic bacteria. Soil Sci. 137, 309–314.
Pugh, C.E., Hossner, L.R., Dixon, J.B., 1981. Pyrite and Marcasite Surface Area as Influenced by Morphology and Particle Diameter1. Soil Sci. Soc. Am. J. 45, 979. doi:10.2136/sssaj1981.03615995004500050033x
Qing You, L., Heping, L., Li, Z., 2006. Study of galvanic interactions between pyrite and chalcopyrite in a flowing system: implications for the environment. Environ. Geol. 52, 11–18. doi:10.1007/s00254-006-0444-5
Rathgeber, C., Yurkova, N., Stackebrandt, E., Beatty, J.T., Yurkov, V., 2002. Isolation of tellurite- and selenite-resistant bacteria from hydrothermal vents of the Juan de Fuca Ridge in the Pacific Ocean. Appl. Environ. Microbiol. 68, 4613–22.
Resing, J.A., Baker, E.T., Lupton, J.E., Walker, S.L., Butterfield, D.A., Massoth, G.J., Nakamura, K., 2009. Chemistry of hydrothermal plumes above submarine volcanoes of the Mariana Arc. Geochemistry, Geophys. Geosystems 10. doi:10.1029/2008GC002141
Resing, J.A., Lupton, J.E., Feely, R.A., Lilley, M.D., 2004. CO2 and 3He in hydrothermal plumes: implications for mid-ocean ridge CO2 flux. Earth Planet. Sci. Lett. 226, 449–464. doi:10.1016/j.epsl.2004.07.028
Richardson, P.E., Yoon, R.-H., Woods, R., Buckley, A.N., 1994. The photoelectrochemistry of galena. Int. J. Miner. Process. 41, 77–97. doi:10.1016/0301-7516(94)90007-8
Ridley, W.I., 2012. Weathering Processes, Volcanogenic massive sulfide occurrence model: U.S. Geological Survey Scientific Investigations Report 2010-5070-C.
Rimstidt, J.D., Chermak, J.A., Gagen, P.M., 1994. Rates of reaction of galena, sphalerite, chalcopyrite, and arsenopyrite with Fe (III) in acidic solutions, in: Alpers, C.N., Blowes, D.W. (Eds.), Environmental Geochemistry of Sulfide Oxidation. American Chemical Society, Washington, DC, pp. 2–13. doi:10.1021/bk-1994-0550.ch001
Rimstidt, J.D., Newcomb, W.D., 1993. Measurement and analysis of rate data: The rate of reaction of ferric iron with pyrite. Geochim. Cosmochim. Acta 57, 1919–1934. doi:10.1016/0016-7037(93)90084-A
Rimstidt, J.D., Vaughan, D.J., 2003. Pyrite oxidation: a state-of-the-art assessment of the reaction mechanism. Geochim. Cosmochim. Acta 67, 873–880. doi:10.1016/S0016-7037(02)01165-1
Romano, G.Y., 2012. Kinetics of Pyrrhotite Oxidation in Seawater: Implications for Mining Seafloor Hotsprings.
Rona, P.A., Thompson, G., Mottl, M.J., Karson, J.A., Jenkins, W.J., Graham, D., Mallette, M., Von Damm, K., Edmond, J.M., 1984. Hydrothermal activity at the Trans-Atlantic Geotraverse Hydrothermal Field, Mid-Atlantic Ridge crest at 26°N. J. Geophys. Res. Solid Earth 89, 11365–11377. doi:10.1029/JB089iB13p11365
Rona, P.A., Trivett, D.A., 1992. Discrete and diffuse heat transfer at ASHES vent field, Axial Volcano, Juan de Fuca Ridge. Earth Planet. Sci. Lett. 109, 57–71.
Rouxel, O., Fouquet, Y., Ludden, J.N., 2004. Copper Isotope Systematics of the Lucky Strike, Rainbow, and Logatchev Sea-Floor Hydrothermal Fields on the Mid-Atlantic Ridge. Econ. Geol. 99, 585–600. doi:10.2113/gsecongeo.99.3.585
Rusanen, L., Aromaa, J., Forsen, O., 2013. Pressure oxidation of pyrite-arsenopyrite refractory gold concentrate.

Physicochem. Probl. Miner. Process. 49, 101–109.
Rzepka, P., Walder, I.F., Aagaard, P., Bożęcki, P., Rzepa, G., 2014. Sub-sea tailings deposition leach modeling. Geol. Geophys. Environ. 40, 123–124.
Sarradin, P.M., Caprais, J.C., Briand, P., 1998. Chemical and thermal description of the environment of the Genesis hydrothermal vent community (13°N, EPR). Cah. Biol. Mar. 39, 159–167.
Sarradin, P.M., Jean-Claude, C., Riso, R., Kérouel, R., Aminot, A., 1999. Chemical environment of the hydrothermal mussel Communities in the Lucky Strike and Menez Gwen vent fields, Mid Atlantic Ridge. Cah. Biol. Mar. 40, 93–104.
Savage, K.S., Stefan, D., Lehner, S.W., 2008. Impurities and heterogeneity in pyrite: Influences on electrical properties and oxidation products. Appl. Geochemistry 23, 103–120. doi:10.1016/j.apgeochem.2007.10.010
Scheirer, D.S., Shank, T.M., Fornari, D.J., 2006. Temperature variations at diffuse and focused flow hydrothermal vent sites along the northern East Pacific Rise. Geochemistry, Geophys. Geosystems 7, 1–23. doi:10.1029/2005GC001094
Schlitzer, R., 2000. Electronic Atlas of WOCE Hydrographic and Tracer Data Now Available. Eos Trans. AGU 81.
Sharkey, J.B., Lewin, S.Z., 1972. Thermochemical properties of the copper(ii) hydroxychlorides. Thermochim. Acta 3, 189–201. doi:10.1016/0040-6031(72)85029-9
Shuey, R.T., 1975. Developments in Economic Geology: Semi-conducting ore minerals. Elsevier Scientific Publishing Company.
Si, R.J., Gu, X.X., Pang, X.C., Fu, S.H., 2006. Geochemical character of dispersed element in sphalerite from Fule Pb–Zn polymetal deposit, Yunnan Province. J. Minerol. Petrol. 26, 75–80.
Simpson, S., Angel, B., Hamilton, I., Spadaro, D., Binet, M., 2007. Water and Sediment Characterisation and Toxicity Assessment for the Solwara 1 Project.
Subrahmanyam, T.V., Forssberg, K.S.E., 1993. Mineral solution-interface chemistry in minerals engineering. Miner. Eng. 6, 439–454. doi:10.1016/0892-6875(93)90173-K
Sui, C.C., Brienne, S.H.R., Ramachandra Rao, S., Xu, Z., Finch, J.A., 1995. Metal ion production and transfer between sulphide minerals. Miner. Eng. 8, 1523–1539. doi:10.1016/0892-6875(95)00116-6
Suzuki, R., Ishibashi, J.-I., Nakaseama, M., Konno, U., Tsunogai, U., Gena, K., Chiba, H., 2008. Diverse Range of Mineralization Induced by Phase Separation of Hydrothermal Fluid: Case Study of the Yonaguni Knoll IV Hydrothermal Field in the Okinawa Trough Back-Arc Basin. Resour. Geol. 58, 267–288. doi:10.1111/j.1751-3928.2008.00061.x
Suzuki, Y., Inagaki, F., Takai, K., Nealson, K.H., Horikoshi, K., 2004. Microbial diversity in inactive chimney structures from deep-sea hydrothermal systems. Microb. Ecol. 47, 186–96. doi:10.1007/s00248-003-1014-y
Tanhua, T., Orr, J., Lorenzoni, L., Hansson, L., 2015. Monitoring Ocean Carbon and Ocean Acidification. WMO Bull. 64.
Taylor, G.F., Scott, K.M., 1982. Evaluation of gossans in relation to lead-zinc mineralisation in the Mount Isa inlier, Queensland. BMRJ. Austr. Geol. Geophys. 7, 159–180.
Taylor, G.F., Thornber, M.R., 1992. The mechanisms of sulphide oxidation and gossan formation, in: Regolith Exploration Geochemistry in Tropical and Subtropical Terrains: Elsevier Handbook of Exploration Geochemistry 4. Elsevier, pp. 119–138.
Thornber, M.R., 1985. Supergene alteration of sulphidesVII. Distribution of elements during the gossan-forming process. Chem. Geol. 53, 279–301. doi:10.1016/0009-2541(85)90075-0
Thornber, M.R., Wildman, J.E., 1984. Supergene alteration of sulphides, VI. The binding of Cu, Ni, Zn, Co and Pb with gossan (iron-bearing) minerals. Chem. Geol. 44, 399–434. doi:10.1016/0009-2541(84)90151-7
Tichomirowa, M., Pelkner, S., Junghans, M., Haubrich, F., Schulz, H.D., Hadeler, A., 2003. Sulfide oxidation at the polymetallic sulfide deposit Freiberg (Germany) and consequences for heavy metal mobilisation., in: Geochemical Processes in Soil and Groundwater: Measurement, Modelling, Upscaling. GeoProc2002 Conference, Bremen, Germany, 4-7 March 2002. Wiley-VCH Verlag GmbH, pp. 356–379.
Tivey, M.A., Dyment, J., 2013. The Magnetic Signature of Hydrothermal Systems in Slow Spreading Environments, in: Rona, P.A., Devey, C.W., Dyment, J., Murton, B.J. (Eds.), Diversity of Hydrothermal Systems on Slow Spreading Ocean Ridges. American Geophysical Union, Washington, D. C. doi:10.1029/2008GM000773
Tivey, M.K., Humphris, S.E., Thompson, G., Hannington, M.D., Rona, P.A., 1995. Deducing patterns of fluid flow and mixing within the TAG active hydrothermal mound using mineralogical and geochemical data. J. Geophys. Res. 100, 12527. doi:10.1029/95JB00610
Tivey, M.K., Stakes, D.S., Cook, T.L., Hannington, M.D., Petersen, S., 1999. A model for growth of steep-sided vent structures on the Endeavour Segment of the Juan de Fuca Ridge: Results of a petrologic and geochemical study. J. Geophys. Res. Solid Earth 104, 22859–22883. doi:10.1029/1999JB900107
Toner, B.M., Rouxel, O., Santelli, C.M., Edwards, K.J., 2008. Sea-floor weathering of hydrothermal chimney sulfides at the East Pacific Rise 9 degrees N: Chemical speciation and isotopic signature of Iron using X-ray absorption spectroscopy and laser-ablation MC-ICP-MS. Geochim. Cosmochim. Acta 72, A951–A951.
Tong, X., Song, S.X., He, J., 2006. Research on mineral processing of marmatite ore. Met. Mine 6, 8–12.
Travis, G.A., Keays, R.R., Davison, R.M., 1976. Palladium and iridium in the evaluation of nickel gossans in Western Australia. Econ. Geol. 71, 1229–1243.
Ueno, H., Hamasaki, H., Murakawa, Y., Kitazono, S., Takeda, T., 2003. Ore and gangue minerals of sulfide chimneys from the North Knoll. JAMSTEC J. Deep Sea Res. 22, 19–62.
Van Dover, C.L., 2014. Impacts of anthropogenic disturbances at deep-sea hydrothermal vent ecosystems: a review. Mar. Environ. Res. 102, 59–72. doi:10.1016/j.marenvres.2014.03.008
Van Dover, C.L., 2010. Mining seafloor massive sulphides and biodiversity: what is at risk? ICES J. Mar. Sci. 68, 341–348. doi:10.1093/icesjms/fsq086
Van Dover, C.L., 2007. The biological environment of polymetallic sulphide deposits, the potential impact of exploration and mining on this environment and data required to establish environmental baselines in exploration areas, in: Polymetallic Sulphides and Cobalt-Rich Ferromanganese Crusts Deposits: Establishment of Environmental Baselines and an Associated Monitoring Programme During Exploration. International Seabed Authority, Kingston, Jamaica, pp. 169–190.
Vanyukov, A.V., Razumovskaya, N.N., 1979. Hydrothermal oxidation of pyrrhotites. Izv. Vyss. Uchelon. Zaved., Tsvetn. Met. 6, 605–610.

Vetriani, C., Chew, Y.S., Miller, S.M., Yagi, J., Coombs, J., Lutz, R.A., Barkay, T., 2005. Mercury adaptation among bacteria from a deep-sea hydrothermal vent. Appl. Environ. Microbiol. 71, 220–226. doi:10.1128/AEM.71.1.220-226.2005
Von Damm, K.L., 1995. Controls on the chemistry and temporal variability of seafloor hydrothermal fluids, in: Seafloor Hydrothermal Systems: Physical, Chemical, Biological, and Geological Interactions. pp. 222–247.
Von Damm, K.L., 1988. Systematics of and postulated controls on submarine hydrothermal solution chemistry. J. Geophys. Res. 93, 4551. doi:10.1029/JB093iB05p04551
Wang, Y., Han, X., Petersen, S., Frische, M., Qiu, Z., Li, H., Li, H., Wu, Z., Cui, R., 2017. Mineralogy and trace element geochemistry of sulfide minerals from the Wocan Hydrothermal Field on the slow-spreading Carlsberg Ridge, Indian Ocean. Ore Geol. Rev. 84, 1–19. doi:10.1016/j.oregeorev.2016.12.020
Wang, Y., Han, X., Petersen, S., Jin, X., Qiu, Z., Zhu, J., 2014. Mineralogy and geochemistry of hydrothermal precipitates from Kairei hydrothermal field, Central Indian Ridge. Mar. Geol. 354, 69–80. doi:10.1016/j.margeo.2014.05.003
Warren, G.W., 1978. The electrochemical oxidation of chalcopyrite. University of Utah, Salt Lake City, Utah.
Warren, G.W., Wadsworth, M.E., El-Raghy, S.M., 1982. Passive and transpassive anodic behavior of chalcopyrite in acid solutions. Metall. Trans. B 13, 571–579. doi:10.1007/BF02650014
Watanabe, S., Hayashi, K., 2014. Mineralogy, Sulfur Isotope and Fluid Inclusion Studies of Hydrothermal Ore at the Hakurei Deposit, Bayonnaise Knoll, Izu-Bonin Arc. Resour. Geol. 64, 77–90. doi:10.1111/rge.12029
Webber, A.P., Roberts, S., Murton, B.J., Hodgkinson, M.R.S., 2015. Geology, sulfide geochemistry and supercritical venting at the Beebe Hydrothermal Vent Field, Cayman Trough. Geochemistry, Geophys. Geosystems 16, 2661–2678. doi:10.1002/2015GC005879
Wei, D., 1996. Semiconductor Electrochemistry of Particulate Pyrite: Dissolution via Hole and Electron Pathways. J. Electrochem. Soc. 143, 3192. doi:10.1149/1.1837186
Weisener, C.G., Smart, R.S.C., Gerson, A.R., 2004. A comparison of the kinetics and mechanism of acid leaching of sphalerite containing low and high concentrations of iron. Int. J. Miner. Process. 74, 239–249. doi:10.1016/j.minpro.2003.12.001
White, S.N., 2009. Laser Raman spectroscopy as a technique for identification of seafloor hydrothermal and cold seep minerals. Chem. Geol. 259, 240–252. doi:10.1016/j.chemgeo.2008.11.008
White, S.N., Kirkwood, W., Sherman, A., Brown, M., Henthorn, R., Salamy, K., Walz, P., Peltzer, E.T., Brewer, P.G., 2005. Development and deployment of a precision underwater positioning system for in situ laser Raman spectroscopy in the deep ocean. Deep Sea Res. Part I Oceanogr. Res. Pap. 52, 2376–2389. doi:10.1016/j.dsr.2005.09.002
Wiersma, C.L., Rimstidt, J.D., 1984. Rates of reaction of pyrite and marcasite with ferric iron at pH 2. Geochim. Cosmochim. Acta 48, 85–92. doi:10.1016/0016-7037(84)90351-X
Williamson, M.A., Rimstidt, J.D., 1994. The kinetics and electrochemical rate-determining step of aqueous pyrite oxidation. Geochim. Cosmochim. Acta 58, 5443–5454. doi:10.1016/0016-7037(94)90241-0
Wohlgemuth-Ueberwasser, C.C., Viljoen, F., Petersen, S., Vorster, C., 2015. Distribution and solubility limits of trace elements in hydrothermal black smoker sulfides: An in-situ LA-ICP-MS study. Geochim. Cosmochim. Acta 159, 16–41. doi:10.1016/j.gca.2015.03.020
Wolfe, A.L., Liu, R., Stewart, B.W., Capo, R.C., Dzombak, D.A., 2007. A method for generating uniform size-segregated pyrite particle fractions. Geochem. Trans. 8, 9. doi:10.1186/1467-4866-8-9
Wolfgram, P.A., Edwards, R.N., Law, L.K., Bone, M.N., 1986. Polymetallic sulfide exploration on the deep sea floor: The feasibility of the MINI‐MOSES experiment. Geophysics 51, 1808–1818. doi:10.1190/1.1442227
Wong, J.W.C., Yang, C.L., 1997. The effect of ph and redox potential on the release of nutrients and heavy metals from a contaminated marine sediment. Toxicol. Environ. Chem. 62, 1–10.
Yelloji Rao, M.K., Natarajan, K.A., 1989. Electrochemical effects of mineral-mineral interactions on the flotation of chalcopyrite and sphalerite. Int. J. Miner. Process. 27, 279–293. doi:10.1016/0301-7516(89)90069-0
Zhang, Q., Xu, Z., Bozkurt, V., Finch, J.A., 1997. Pyrite flotation in the presence of metal ions and sphalerite. Int. J. Miner. Process. 52, 187–201. doi:10.1016/S0301-7516(97)00064-1
Zierenberg, R.A., Shanks, W.C., 1983. Mineralogy and geochemistry of epigenetic features in metalliferous sediment, Atlantis II Deep, Red Sea. Econ. Geol. 78, 57–72. doi:10.2113/gsecongeo.78.1.57
Zierenberg, R.A., Shanks, W.C., Bischoff, J.L., 1984. Massive sulfide deposits at 21N, East Pacific Rise: Chemical composition, stable isotopes, and phase equilibria. Geol. Soc. Am. Bull. 95, 922–929. doi:10.1130/0016-7606(1984)95

10 Figure Captions

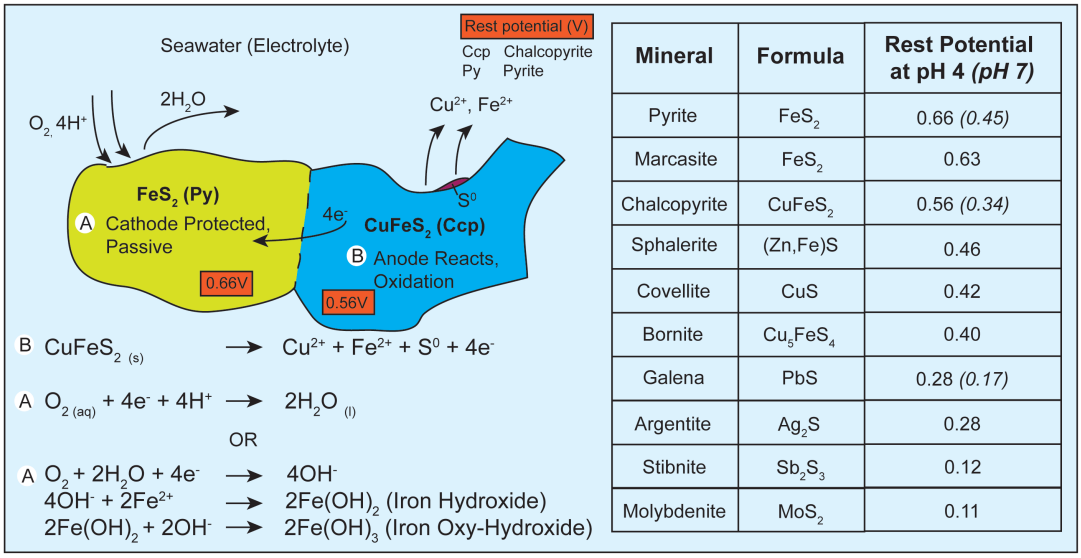

Mineral	Formula	Rest Potential at pH 4 *(pH 7)*
Pyrite	FeS_2	0.66 *(0.45)*
Marcasite	FeS_2	0.63
Chalcopyrite	$CuFeS_2$	0.56 *(0.34)*
Sphalerite	(Zn,Fe)S	0.46
Covellite	CuS	0.42
Bornite	Cu_5FeS_4	0.40
Galena	PbS	0.28 *(0.17)*
Argentite	Ag_2S	0.28
Stibnite	Sb_2S_3	0.12
Molybdenite	MoS_2	0.11

Figure 1

A galvanic cell occurs when two sulphide minerals with different rest potentials are coupled together in a solution that acts as an electrolyte (seawater in this case). The mineral with the higher rest potential behaves as a cathode (e.g. pyrite) and is galvanically protected with the reduction reaction occurring on its surface. The mineral with the lower rest potential (e.g. chalcopyrite) behaves as an anode and is preferentially dissolved with oxidative dissolution occurring on its surface. There are a number of potential reduction reactions that occur on the surface of the cathode depending on the ions available; shown above are the formation of water as well as hydroxides that can then ultimately form iron hydroxides/oxy-hydroxides if ferrous iron is available. Figure adapted from Murr (2006). Rest potentials of minerals at pH 4 are taken from Majima (1969) and references therein; quoted where available are rest potentials of minerals at pH 7 in distilled water, taken from Cheng and Iwasaki (1992).

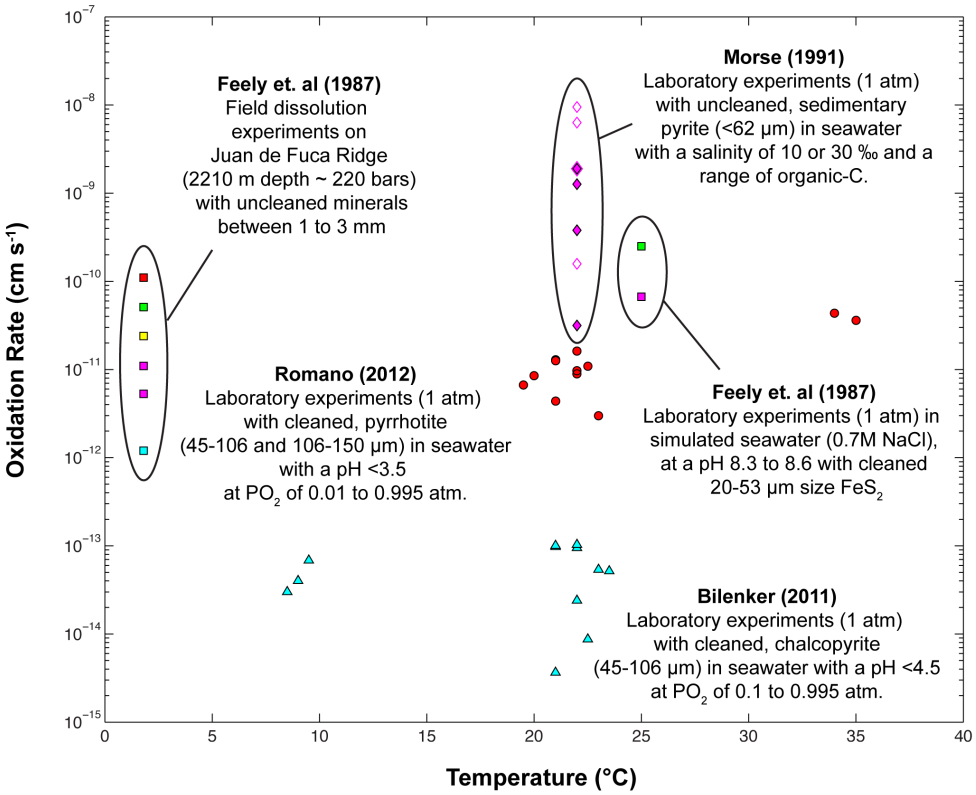

Figure 2

The oxidation rates of individual sulphide minerals in cm s^{-1} versus temperature. Colour denotes sulphide mineral; magenta: pyrite, green: marcasite, yellow: sphalerite, cyan: chalcopyrite and red: pyrrhotite. Shape denotes the study; squares: Feely et al. (1987), diamonds: Morse (1991), circles: Romano (2012) and triangles: Bilenker (2011). Rates in cm s^{-1} for Bilenker (2011) and Romano (2012) were calculated using raw mol/kg/sec, area/volume (A/V) and surface area data provided (as well as the molecular mass (Mr) of Cu/Fe and density of chalcopyrite and pyrrhotite). Rates in cm s^{-1} for Morse (1991) were calculated using raw data from Morse (1991), and applying a second order polynomial fit to provide a rate in mol/kg/sec. A subsequent rate in cm s^{-1} (shown here) was calculated (Appendix A) using the Mr, density of pyrite and a maximum and minimum surface area sourced from the literature (as none was provided) (Pugh et al., 1981; Wiersma and Rimstidt, 1984; Wolfe et al., 2007) to show a range. Rates derived using a minimum surface area of 0.3 m^2/g are shown as unfilled diamonds, versus maximum surface area of 1.5 m^2/g shown as filled diamonds. The rates derived using the larger surface area are shown to be

more comparable with the mol/kg/sec data (see Appendix A). Oxidation rates were achieved over a range of different variables outlined in the figure.

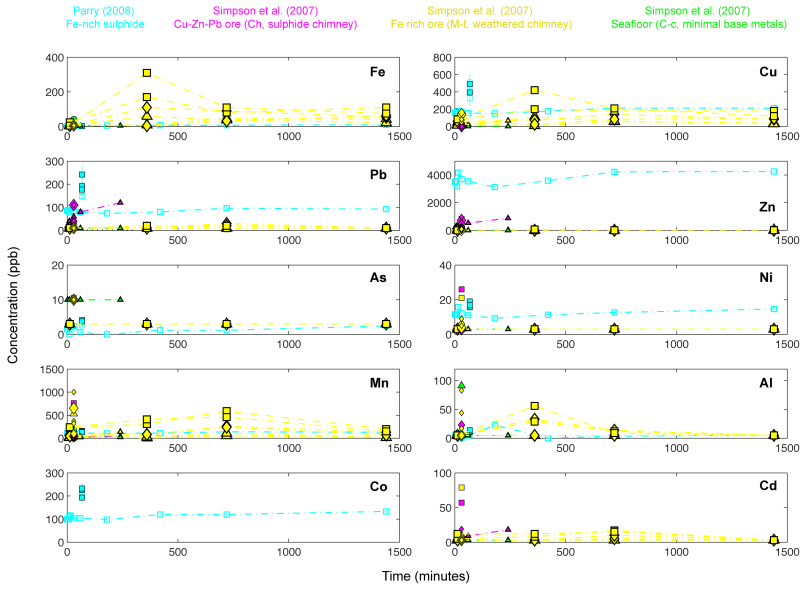

Figure 3

The concentrations of total dissolved metals (ppb) in elutriate waters (<0.45 um filtered) leached over time. Colour dictates the ore type; blue: ore from Parry (2008), yellow: weathered chimney (M-t), magenta: chimney (Ch), green: seafloor sediment (C-c). Filled symbols denote experiments undertaken at temperatures >20°C, unfilled: ≤12°C. Shapes denote fluid to rock ratio: circle: 1g/L, triangle: 10g/L, diamond: 40g/L and square: 90-100g/L. Marker size indicates grain size; small: <1mm, medium: 1- 4mm, large: >4mm. Data presented from EIS reports (Parry, 2008; Simpson et al., 2007) are quoted in Appendix B.

Graphical Abstract